Evolution of symbiotic interactions to enhance aphid transmission of plant viruses and satellite RNAs

ウイルスやそのサテライト RNA のアブラムシ伝搬を促進する共生相互作用の進化

Hokkaido University Graduate School of Agriculture

Division of Agrobiology Doctor Course

Wikum Harshana Jayasinghe

CONTENTS

LIST OF FIGURES

LIST OF TABLES

ABBREVIATIONS

OYDV	Onion yellow dwarf virus
OYDV-L	Onion yellow dwarf virus isolates with intact HC-Pro
OYDV-S	Onion yellow dwarf virus isolates with mutated HC-Pro
LYSV	Leek yellow stripe virus
HC-Pro	Helper component protease
CP	Coat protein
CMV	Cucumber mosaic virus
Y-sat	Y-satellite RNA

GENERAL INTRODUCTION

Plant viruses make two kinds of movements in its life cycle. One is the movement within the plant from the initial infection point and the second is from one host plant to another. For the later, most viruses seek assistance of insects and mostly Hemipteran insects play an important role in this regard. Aphids with their unique morphological and physiological characters have become the most important plant virus vector. They are responsible for the transmission of nearly 40% of all known plant viruses.

Aphid transmission of plant viruses can be categorized as non-persistent, semi-persistent, or persistent transmission (Watson and Roberts 1939; Sylvester 1956). Persistent viruses pass through cellular barriers and enter the aphid body while both non-persistent and semi-persistent viruses are confined into the aphid stylet (Kennedy et al. 1961a; Pirone and Harris 1977; Harris 1977). Persistent viruses can be further categorized in to two groups; persistent-propagative and persistent-non-propagative based on the virus's ability to replicate within the insect body. These viruses are also known as circulative-propagative and circulative-non-propagative, respectively.

Non-persistent and non-circulative viruses are also known as stylet-borne/cuticle-borne viruses. These viruses never pass-through cellular barriers of the insect. At the molecular level, these viruses use two distinct modes to bind to the insect stylet, i.e., capsid strategy and helper strategy. An insect stylet processes receptor proteins for these viruses and in the capsid strategy, virus coat proteins can directly bind to those stylet receptors. Other viruses use a helper protein to link the coat protein and stylet receptor protein. The later mode of transmission is known as helper strategy, which has been explained by the bridge hypothesis (Pirone and Blanc 1996). All potyviruses are thought to be aphid transmitted in a non-persistent manner using the helper strategy.

Viruses are sometimes found to be associated with subviral non-cording RNA molecules, which are known as satellite RNAs. This non-cording RNA has been found to play an important role in

plant-virus-vector interactions (Simon et al. 2004; Roossinck 2005). Satellite RNA can modify the viral accumulation levels and the symptoms caused by the helper virus (Shimura et al. 2011).

Coevolution is a major model for research on the evolution of symbiotic interactions between species in an ecosystem. The prevailing view is that natural selection within local populations is the major evolutionary process driving this form of coevolution. In the processes of evolution, all living beings, even the simplest organisms coevolve by many means for its survival in the nature. The idea of onward transmission is indispensable for the survival of plant viruses and satellite RNAs.

In this thesis, two symbiotic interactions for coevolution among plant viruses to promote aphid transmissibility have been documented. The chapter one explains how an onion dwarf virus isolate with a mutated HC-Pro gene, which has lost the ability to transmit via aphids, have coevolved a symbiotic relationship with another potyvirus, leek yellow stripe virus (LYSV) to regain aphid transmissibility. It was experimentally shown that LYSV HC-Pro works *in trans* as a platform that interlinks both LYSV and OYDV-S to the aphid stylet. In the chapter two, an extraordinary survival strategy mediated by a non-coding RNA is presented. In this chapter, the coevolution of a symbiotic interaction among Y-satellite RNA, cucumber mosaic virus, tabaco plant and aphid is explained.

Chapter 1: Helper component protease (HC-Pro) of leek yellow stripe virus facilitates the aphid transmission of an onion yellow dwarf virus isolate with a mutated HC-Pro gene: A symbiotic association evolved among two potyviruses

INTRODUCTION

Role of HC-Pro of potyviruses in the bridge hypothesis

The helper phenomenon was first described by Kassanis and Govier (Raccah et al. 2001); it was noted that aphid transmission of potyviruses occurs only if the virus is acquired along with or after the acquisition of a special helper protein, later known as HC-Pro. The observation that the helper component (HC) binds to aphid mouthparts and virions bind to the HC, led to the bridge hypothesis. The domains involved in vector transmission were identified by using virus isolates with active and inactive HC. The conserved KITC motif in the N-terminal region of HC-Pro is important for aphid transmission (Blanc et al. 1998). Another conserved motif in the central region of the HC-Pro gene, PTK, was found to affect the HC's binding to virions (Raccah et al. 2001).

Virus infection in garlic

Garlic (*Allium sativum*) is a popular condiment and has always been used as a medicine in many societies. Thus, garlic is grown in almost all the countries. Garlic cultivation is wholly dependent on vegetatively propagated planting material. Nevertheless, different types are available, differing by the size and colour of bulbs and the adoptability to climatic conditions (Pitrat 2012).

In garlic, we frequently detect in mixed infections with *Potyvirus*, *Carlavirus* and *Allexivirus*. OYDV and LYSV, which are members of *Potyvirus* are the most common viruses of garlic (Mohammed et al. 2013; Manglli et al. 2014). In a survey conducted by Van Dijk (1996) found that 73% and 45% garlic propagative material collected from all over the world are infected with OYDV and LYSV, respectively. OYDV infection in garlic causes dwarfing of the plant growth and curled leaves with irregular yellow stripping (Arya et al. 2006) while LYSV infection results in distinct yellow stripes. In garlic, OYDV is frequently found in a mixed infection with LYSV and allexiviruses, and sometimes also with carlaviruses. This mixed infection synergistically produces more severe symptoms and heavy yield losses (Lot et al. 1998).

Both OYDV and LYSV are transmitted by aphids in a nonpersistent manner. *Myzus persicare* is an efficient vector for the both viruses. OYDV and LYSV are not seed-borne. Under the laboratory conditions, mechanical transmission of both viruses were successful for a number of plant species (Katis et al. 2012).

HC-Pro mutation in OYDV isolate from garlic from Hokkaido, Japan

It has been previously reported that garlic plants in Aomori Prefecture, Japan were infected with a spontaneous mutant of the OYDV, which was named as isolate G79. This OYDV isolate lacks 92 amino acids in the N-terminal of HC-Pro (Takaki et al. 2006). In a recent survey using garlic cultivated in Hokkaido and a few other regions in Japan, we found that OYDV was always associated with LYSV in garlic. In the sequence information of several HC-Pro genes from OYDV isolates from Japanese garlic showed that all of the HC-Pro proteins lacked about 100 amino acids in the N-terminal region (Kim et al. 2020). The OYDV isolates with an N-terminal deletion (about 100 amino acids) are hereafter called OYDV-S in this report. In a phylogenetic tree constructed based on the HC-Pro amino acid sequences showed that the OYDV isolates are divided into three distinct groups (Group I–III). It was also identified that the mutated HC-Pro was originated from an ancestor containing a long type HC-Pro (Kim et al. 2020).

Japanese OYDV may have lost aphid transmissibility

Several studies conducted with tobacco etch virus and tobacco vein mottling virus have revealed that the KITC motif in HC-Pro N-terminal is absolutely necessary for aphid transmission (Atreya and Pirone 1993; Blanc et al. 1998). Since the missing sequences of N-terminal of HC-Pro of the OYDV isolated form Japanese garlic include the KITC motif, it is assumed that those isolates have lost the ability to be aphid transmissible (Kim et al. 2020). The OYDV isolates without a deletion at the N-terminus (intact HC-Pro) should be transmitted by aphids. These OYDV isolates with an intact HC-Pro are hereafter called OYDV-L in this report. Considering that OYDV-S was

always associated with LYSV, it was hypothesised that OYDV-S strains may be transmitted by aphids only when they are coinfecting garlic with LYSV.

MATERIAL AND METHODS

Plant material and insect stock

Garlic bulbs, which had been sold commercially as virus-free, were purchased and checked for LYSV, OYDV, allexiviruses, garlic latent virus [GLV] and garlic common latent virus [GCLV]) by RT-PCR. These bulbs were sown on potting material to obtain seedlings. For onion, commercially available onion seeds were purchased and sown, and the seedlings were grown in a plant incubator with 16-h light/8-h dark at 24°C.

Colonies of *Myzus persicae* (Sulzer) (Insecta: Hemiptera: Aphididae) originally isolated from *Nicotiana tabacum* were reared on *Brassica rapa* in the laboratory at 24°C under artificial light with photoperiod of 16hrs.

Virus inoculum preparation

OYDV-L: Previously identified OYDV-L isolate (isolate America) originally isolated from America garlic (Kim et al. 2020) was maintained in garlic by rub-inoculation.

OYDV-S: Previously identified OYDV-S isolate (isolate Hakko) originally isolated from Hokko garlic (Kim et al. 2020) was maintained in garlic by rub inoculation. Sap from OYDV-S and LYSV mixed infected garlic plant was rub-inoculated into four virus free onion seedlings (Cultivar: Kitano-Daichi). Fourteen dpi, the upper non-inoculated leaves of onion seedlings were tested for OYDV, LYSV, allexiviruses, GCLV and GLV. After confirming that the onion tissue is only infected with OYDV-S, this sap was then rub-inoculated into virus free garlic. Successfully infected plants were again confirmed to be free from LYSV, allexiviruses, GCLV and GLV by RT-PCR. Figure 1 shows the schematic diagram of the above methodology.

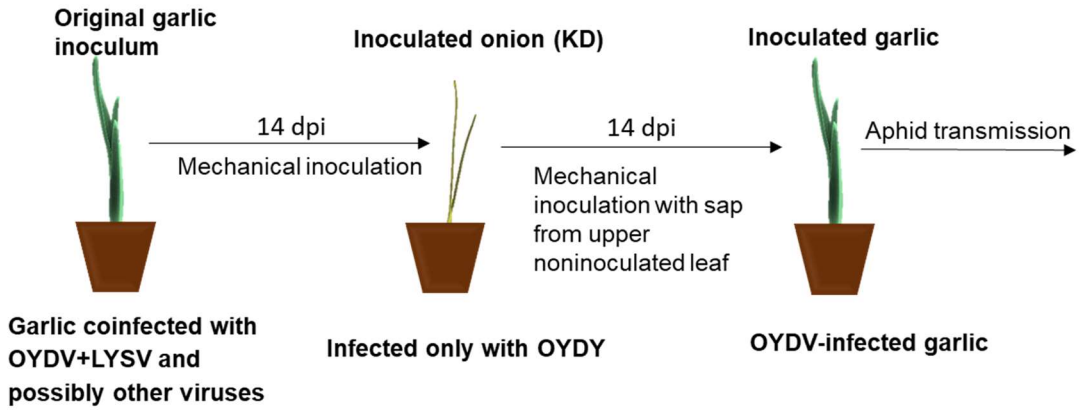

Figure 1 Strategy to obtain OYDV-only-infected plants from mixed-infected garlic

[OYDV-S+LYSV] mixed-inoculum: previously identified [OYDV-S+LYSV] (Kim et al. 2020) was maintained in garlic by rub-inoculation.

[OYDV-L+LYSV] mixed-inoculum: previously identified [OYDV-L+LYSV] isolate (Kim et al. 2020) was maintained in garlic by rub-inoculation.

Aphid transmission assay

In the experiment 1, aphid transmission was done from garlic plants coinfected with OYDV-S and LYSV to eighteen virus-free garlic plants. In the experiment 2, aphid transmission was done from OYDV-S-only-infected garlic and onion plants to 16 and 14 virus-free garlic plants, respectively. Finally, in the experiment 3, aphid transmission was done from OYDV-L-infected garlic to ten virus-free garlic and six virus-free onion plants. Furthermore, aphid transmission was done from OYDV-L-infected onion to seven virus-free garlic plants. Aphid transmission was done as follow.

Ten aphids per plant were used for the test. To assess virus-transmission frequency by *M. persicae,* apterous aphids, which had been starved for 5 h, were allowed a 2–5-min acquisition access period

on the inoculum-source plant. Aphids that had test-probed leaves were then collected and transferred to virus-free test plants using a fine dry paintbrush and allowed an inoculation access period of 24 h. Aphids were then killed using a systemic pesticide (Orutorun, Sumitomo Chemical, Co).

RT-PCR

Total RNA from plant tissues were extracted using tryzol following the manufactures protocol. The total RNA extracted were used as the template for cDNA synthesis by RT-PCR. Primers used for LYSV, OYDV, allexiviruses, GLV and GCLV are shown in Table 1.

Table 1. List of primers used for virus detection

Virus	Primer Name	Primer Sequence (5' - 3')
LYSV	LT5P	AATCTCAACACAACTTATRC
	LY2M	AGTACGTTGCCTGCTCTGTAG
OYDV	OYDV-CP-FW1	AATTGGACAATGATGGACGG
	OYDV-CP-RV1	GTTACCATCCAGGCCAAACA
Allexivirus	al-CP5-750	TGGRCNTGCTACCACHHYGG
	al-CP3-750	CCYTTCAGCATATAGCTTAGC
GLV	GLV-5-1000	AGGTGCATTGTTATCATTACTGG
	GLV-3-1000	GTATGCAACTTAAATATAGCACGC
GCLV	GCLV-5-1070	GCTAGACATTGGTAGCCTTAGG
	GCLV-3-1070	GTCAGTAGGCACGCCACTAT

Pull-down assay with His-affinity gel

For the transient overexpression of LYSV HC-Pro and OYDV CP in *N. benthamiana*, the LYSV HC-Pro and OYDV CP genes were first cloned into the pBE2113 binary vector. The N-terminal His-tag sequence was added to HC-Pro. The C-terminal FLAG-tag sequence was added to both HC-Pro and CP. *Agrobacterium* cells were then transformed with those vectors and used for the conventional agroinfiltration. Briefly, the bacterial cells in the resuspension buffer (10 mM MES, 10 mM $MgCl_2$ and 200 μM acetosyringone) at OD_{600} of 1.0 were infiltrated into *N. benthamiana* leaves using 1 ml syringe without needle. The infiltrated leaf tissues were taken at 2 days post agroinfiltration and ground by mortar and pestle in 0.3 M potassium phosphate buffer (pH 8.0). The soluble fraction of the plant extracts was separated by centrifugation at 2000 *g* for 10 min at 4℃. The His-tagged LYSV HC-Pro proteins were pulled down using the His-Spin Protein Miniprep kit (Zymo Research) following the manufacturer's instruction. The purified proteins were separated by SDS-PAGE in a 10% polyacrylamide gel, and then the OYDV CP was detected by Western blot analysis using anti- OYDV CP antibodies.

Production of the N-terminal MBP-fused proteins in *E. coli*

The coding cDNA sequences of OYDV CP, LYSV HC-Pro and LYSV HC-Pro mutants (MBP-HC900, MBP-HC700 and MBP-HC460*)* (Fig. 2) were cloned into the plasmid, pMAL-c2x (New England Biolabs, NEB). The HC-Pro proteins contain the C-terminal FLAG-tag. The transformants of *E. coli* strain BL21 were grown in the rich and glucose medium (RGM) and harvested by centrifugation. The cells were broken by sonication, and the soluble fractions were collected by centrifugation at 4 ℃ for 20 min. The MBP-fused proteins were purified through the column following the manufacturer's instruction. Briefly, the protein extracts in the soluble fraction were co-incubated with amylose resin (NEB) at 4 ℃ for 1 h with rotation and loaded onto the column. The MBP-CP, MBP-HC-Pro and MBP-HC-Pro deletion mutants were eluted in the 10 mM maltose solution after washing with the column buffer (3M NaCl, 2-mercaptoethanol, 0.5 M sodium phosphate, pH 7.2).

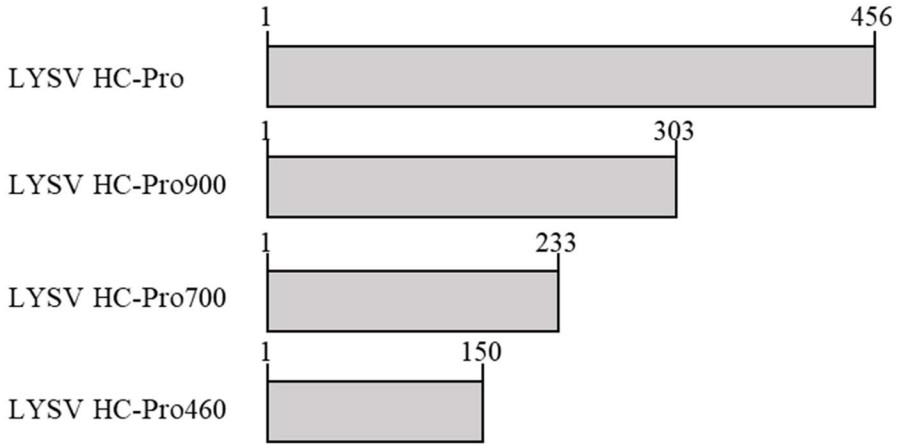

Figure 2 Schematic representation of the MBP-HC-Pro and its deletion mutants (MBP-HC900, MBP-HC700 and MBP-HC460). The amino acid residue numbers are indicated above the boxes.

Far-Western dot blot analysis

The Far-Western dot blot analysis was carried out as followed. MBP-CP (1 μg) was dot-blotted onto a nitrocellulose membrane and then dried. The membrane was soaked into TBS (Tris-Buffered Saline) with 5% BSA for 30 min with agitation. When HC-Pro was used as a probe, the FLAG-tagged MBP-HC-Pro and FLAG-tagged MBP-HC-Pro deletion mutants (MBP-HC900, MBP-HC700 and MBP-HC460) (10 μg/ml) was overlaid on the dots by incubating the membrane in the TBS for 2 h at room temperature. After washing in TBS, the membrane was incubated with anti-FLAG monoclonal antibody (Fujifilm, 1:3000 dilution) for 30 min, followed by washing in TBS-T (Tris-Buffered Saline with Tween 20). The secondary antibody reaction was then performed by incubating the membrane with the anti-mouse IgG-alkaline phosphatase conjugate (Sigma, 1:5000 dilution) for 30 min. After washing in TBS-T, the probe proteins were detected in an alkaline phosphatase reaction in LAS4000 (Fujifilm). When CP was used as a probe, MBP-OYDV CP was first labeled with biotin using the biotin labeling kit (Dojindo Molecular

Technologies) following the manufacturer's instruction. The MBP-HC-Pro and its deletion mutants (MBP-HC900, MBP-HC700 and MBP-HC460) were first dot-blotted onto nitrocellulose membrane. After blocking the membrane in TBS with 5% BSA, the biotin-labelled CP probe (10 μg/ml) was overlaid on the dots by incubating the membrane overnight at room temperature. After washing in TBS, the membrane was incubated with the streptavidin-alkaline phosphatase conjugate (Bio-rad, 1:2000 dilution). The signals were detected as above.

RESULTS

Viruses detected in the sap from plants used for inoculum

All plants used as inoculum was tested for OYDV, LYSV, allexiviruses, GCLV and GLV. The results are shown in the Table 2.

Table 2. Viruses detected in the plants used as an inoculum

	Inoculum	Viruses detected				
		OYDV	LYSV	Allexivirus	GCLV	GLV
Exp. 1	Garlic	+	+	–	–	–
Exp. 2	Garlic	+	–	–	–	–
	Onion	+	–	–	–	–
Exp.3	Garlic	+	–	–	–	–
	Onion	+	–	–	–	–

+, virus detected; –, not detected

Aphid transmission assay

In the experiment 1, of 18 tested plants, 9 plants were infected only with LYSV, while 3 plants were coinfected with LYSV and OYDV-S. No plants were infected with only OYDV-S. All 18 tested plants tested negative for allexiviruses, GCLV and GLV (Table 3).

Table 3. Aphid transmission of mix-infected OYDV-S and LYSV

	Inoculum (Virus)	Inoculated plants[a] (Number)	No. of infected plants (Percentage)				
			OYDV	LYSV	Allexivirus	GCLV	GLV
Exp. 1	Garlic (OYDV-S +LYSV)	Garlic (18)	3[b] (17%)	11 (61%)	–	–	–

–, not detected; nt, not tested

OYDV-S, OYDV with short HC-Pro; OYDV-L, OYDV with long HC-Pro

[a]These plants were virus free

[b]These plants were co-infected with LYSV and OYDV-S

To conduct the experiment 2, OYDV-S-only-infected garlic was prepared as explained in the methods. Of 4 inoculated onion plants, 2 tested were positive for OYDV-S and free of LYSV. Subsequently, the inoculated garlic plants tested positive for OYDV-S and negative for LYSV, allexiviruses, GCLV and GLV (Table 2).

Both garlic and onion were used as inoculum source plants in separate studies. The RT-PCR results showed that all tested garlic plants were not infected. Sixteen test plants, where garlic was used as inoculum source, also tested for allexivirus and showed none of the plants were infected with allexiviruses. The onion inoculum source plant tested negative for LYSV, allexiviruses, GCLV and GLV (Table 4).

In the experiment 3, OYDV-L transmitted from the infected garlic to 10 virus free garlic, three garlic and out of six onion, one plant tested positive. When OYDV-L was aphid transmitted from onion to garlic, of seven tested garlic two tested positive for OYDV (Table 5).

Table 4. Aphid transmission of OYDV-S from OYDV-S only infected plants

	Inoculum (Virus)	Inoculated plants[a] (Number)	No. of infected plants (Percentage)				
			OYDV	LYSV	Allexivirus	GCLV	GLV
Exp. 2	Garlic (OYDV-S)	Garlic (16)	–	–	–	Nt	nt
	Onion (OYDV-S)	Garlic (14)	–	–	Nt	Nt	nt

–, not detected; nt, not tested
OYDV-S, OYDV with short HC-Pro; OYDV-L, OYDV with long HC-Pro
[a]These plants were virus free

Table 5. Aphid transmission of OYDV-L

	Inoculum (Virus)	Inoculated plants[a] (Number)	No. of infected plants (Percentage)				
			OYDV	LYSV	Allexivirus	GCLV	GLV
Exp.3	Garlic (OYDV-L)	Garlic (10)	3 (30%)	–	–	–	–
		Onion (6)	1 (17%)	–	Nt	Nt	nt
	Onion (OYDV-L)	Garlic (7)	2 (29%)	–	Nt	Nt	nt

–, not detected; nt, not tested
OYDV-S, OYDV with short HC-Pro; OYDV-L, OYDV with long HC-Pro
[a]These plants were virus free

Semi-quantitative RT-PCR

Semi-quantitative RT-PCR results showed that the viral accumulation levels are comparable between OYDV-S-only-infected-Hakko garlic and OYDV-S+LYSV-mixed-infected-China garlic. The accumulation level in Hokkaido garlic, which was infected with both viruses (OYDV-L+LYSV), was even lower than that in Onion infected only with OYDV-S (Fig. 3).

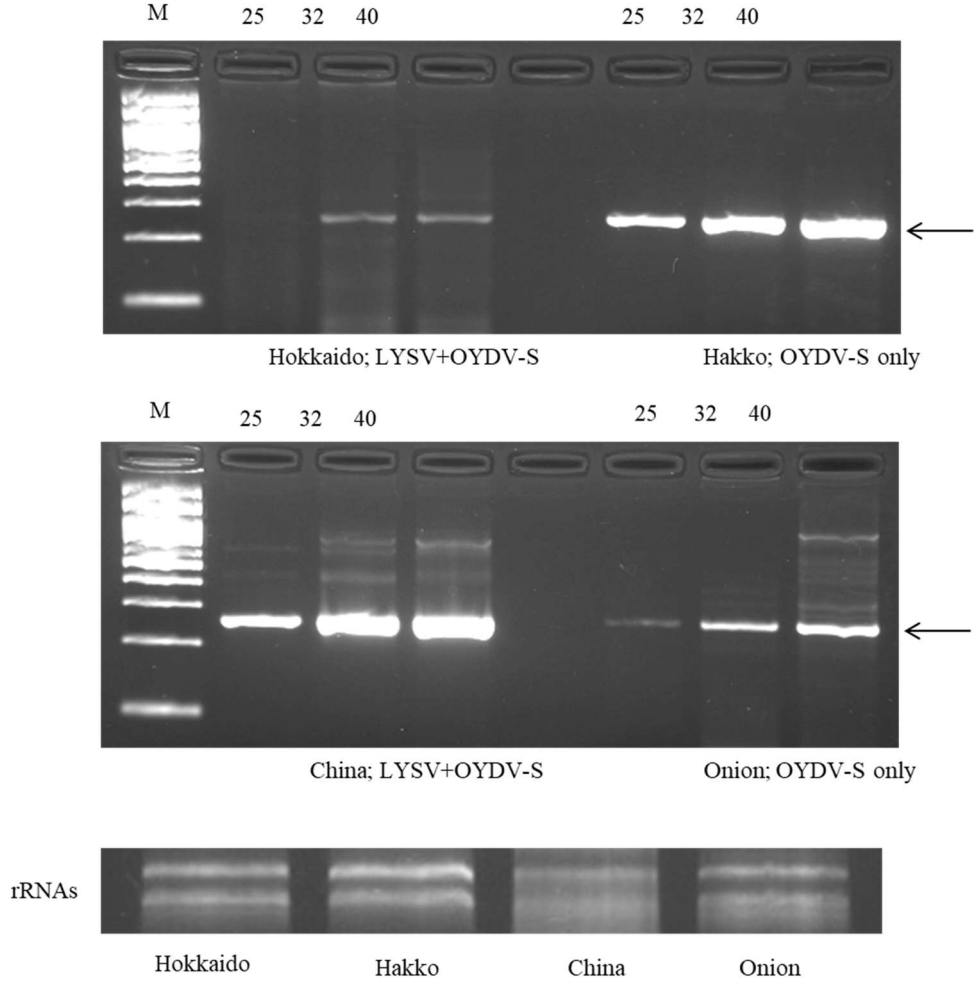

Figure 3 Semi-quantitative RT-PCR analysis of the OYDV RNA. The Hakko garlic and onion plants were the inoculum plants in Table 4 and infected only with OYDV-S. The Hokkaido and China garlic plants were infected with both LYSV and OYDV-S. The arrow indicates the specific PCR product for OYDV. To estimate the relative input RNA abundances used for the reverse transcription, ribosomal RNAs (rRNAs) of each sample were detected by ethidium bromide staining (bottom panel). The PCR cycles are indicated above each lane.

Pull-down assay with His-affinity gel

The input proteins used for the pull-down assay were detected on Western blots (Fig. 4). The HC-Pro and CP bands are indicated by arrows in Fig. 4. As shown in Fig. 5, the OYDV CP was detected in the pull-down fraction of HC-Pro.

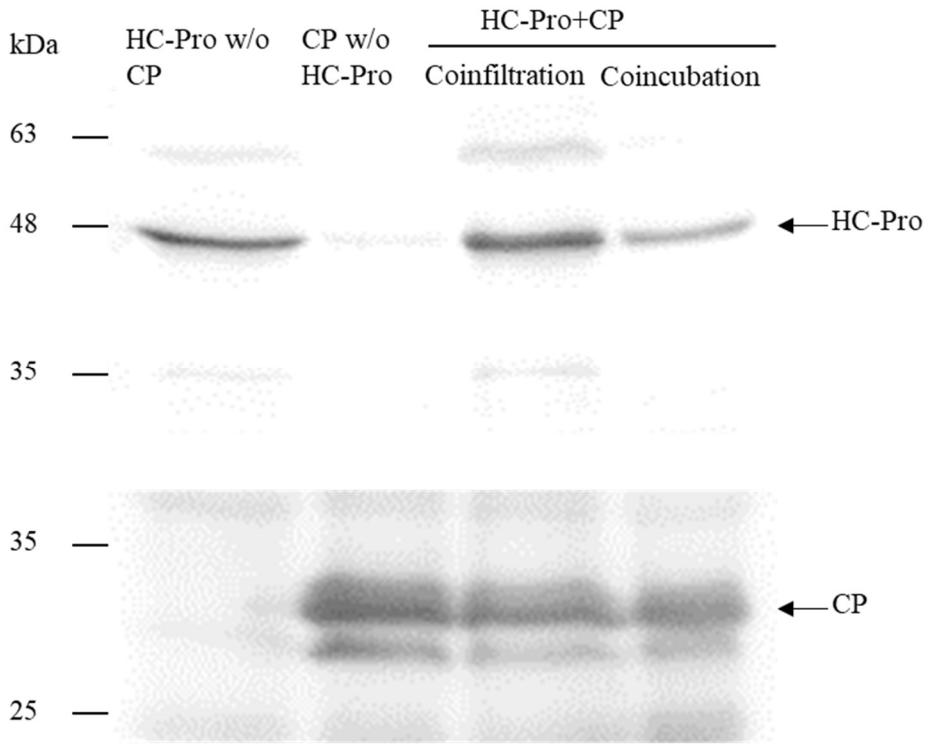

Figure 4 The input proteins used for the pull-down assay were detected on Western blots. The HC-Pro and CP bands are indicated by arrows.

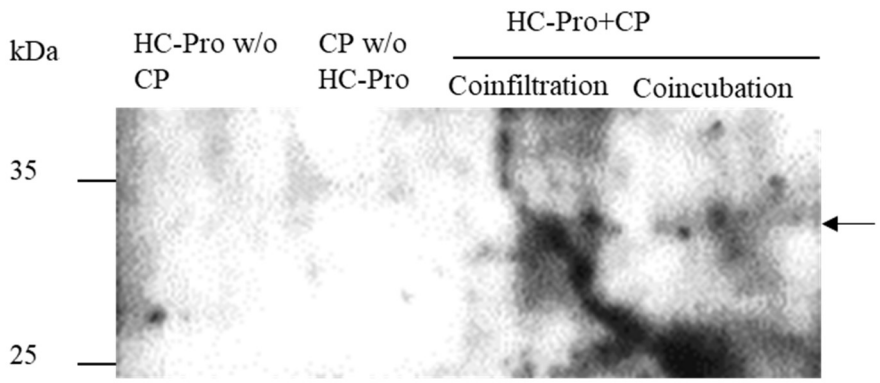

Figure 5 Pull-down assay with His-affinity gel. LYSV HC-Pro was expressed in the agrobacterium-infiltrated Nicotiana benthamiana leaf tissues, harvested 2 days after infiltration and pulled down using the nickel-charged His-Affinity Gel (Zymo Research). The two proteins were synthesized either in the same leaf tissues (coinfiltration) or in different tissues whose plant extracts were mixed (coincubation) and incubated for 30 min before pull-down. The detected CP band was indicated by arrow.

Far-Western dot blot assay

The results showed that HC-Pro and CP bound to each other in a reciprocal combination (Fig. 6).

The input is shown in the figure 7.

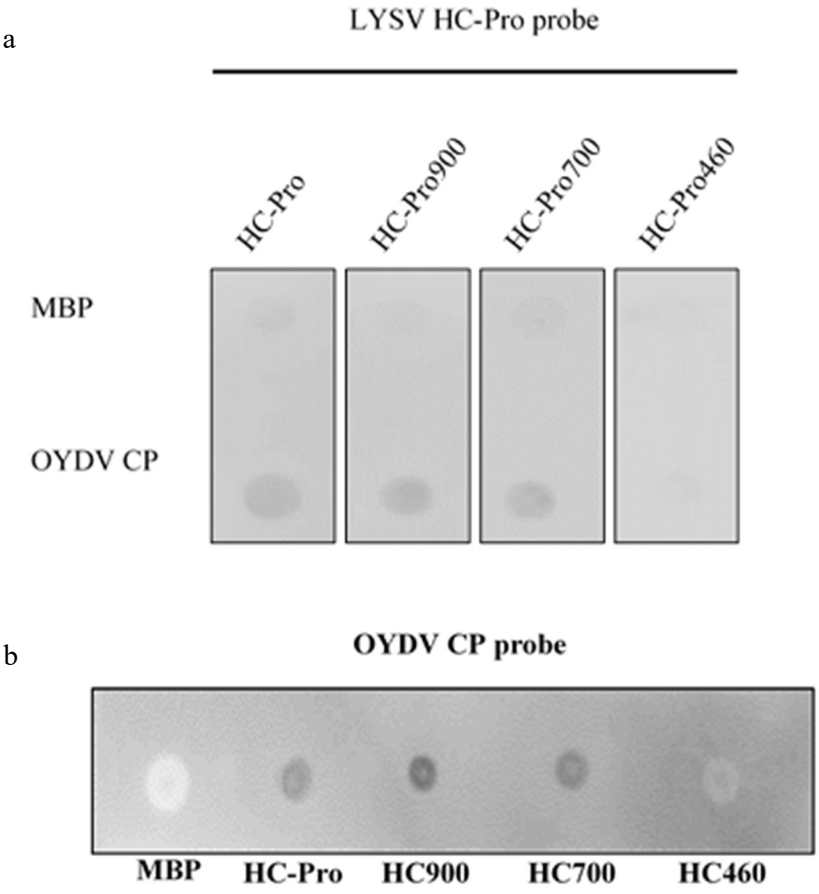

Figure 6 Far-Western dot blot analysis. a, OYDV CP-MBP was dotted onto the nitrocellulose membrane, overlaid with the MBP-C-terminal truncated LYSV HC-Pro proteins. The signals were detected by incubating the blots with mouse anti-flag antibody followed by anti-mouse alkaline phosphatase conjugate. b, The MBP-C-terminal truncated LYSV HC-Pro proteins were dotted onto the nitrocellulose membrane, overlaid with the MBP-OYDV CP. The signals were detected by incubating the blots with rabbit anti-OYDV CP antibodies followed by anti-rabbit alkaline phosphatase conjugate.

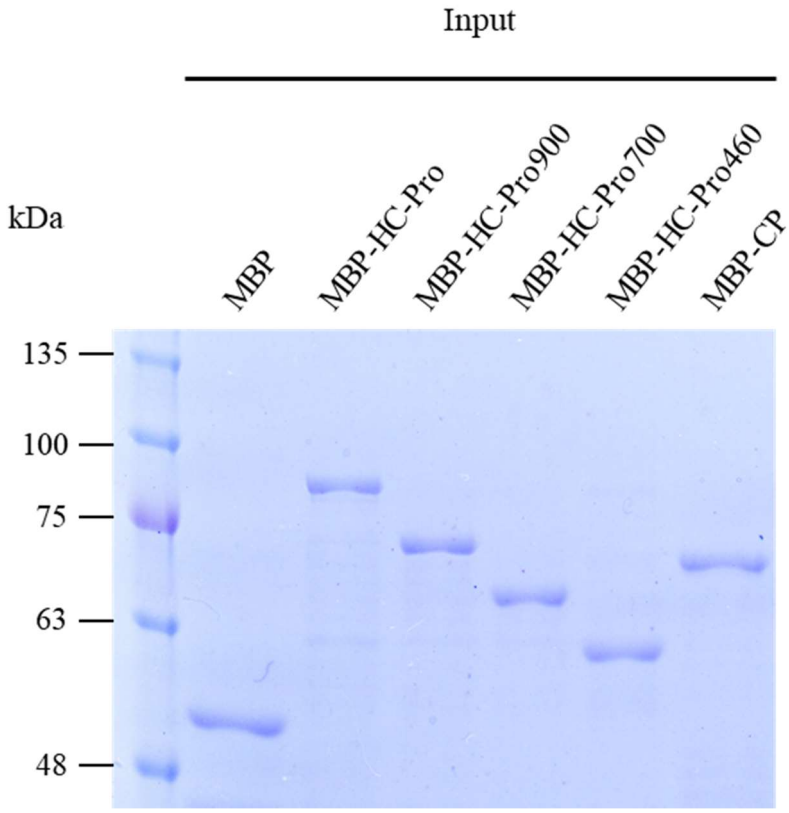

Figure 7 The input of MBP fusion proteins used for the Far-Western dot blot analysis.

DISCUSSION

As previously reported, the deletion region on N-terminus contains the KITC motif important for aphid transmission and therefore the OYDV with short-type HC-Pro is considered to have lost its aphid transmissibility. Kim et al. (2020) found that all investigated isolates of OYDV-S from Hokkaido garlic were co-infected with LYSV and hypothesised that the HC-Pro of LYSV might help OYDV-S to be transmitted by aphids.

To test this hypothesis, experiments were designed to clarify whether i) OYDV-S is transmitted by aphids, ii) OYDV-S is transmitted by aphids when mixed-infected with LYSV and iii) OYDV-L alone is transmitted by aphids.

Garlic bulbs, which had been sold commercially as virus-free were purchased and confirmed that those were not infected with LYSV, OYDV, allexiviruses, GLV and GCL by RT-PCR. Virus-free onion were obtained from planting seeds. The biggest challenge was to acquire plants infected only with OYDV for the aphid transmission tests. The most reliable method was to use onion as an intermediate propagation host. Onions are easily infected with OYDV but rarely infected by LYSV. Allexiviruses and carlaviruses (GCLV and GLV) also rarely infect onion although some onion cultivars have been reported to be susceptible to these viruses (Ward et al. 2009). Using onion as an intermediate host have some advantages because onion is grown from seeds, making it easier to prepare virus-free seedlings, and seedlings are able to mechanically inoculated about 10 days after sowing.

Initially, aphid transmission from garlic plants coinfected with OYDV-S and LYSV to virus-free garlic plants was tested. As shown in Table 3, the RT-PCR results showed that the infection rates of LYSV and OYDV-S were 61% and 17%, respectively. No plants were infected only with OYDV-S.

In the experiment two, the RT-PCR results revealed that OYDV-S was not transmitted to any of the tested garlic plants regardless of the inoculum source plant (Table 4). On the other hand, aphids could transmit OYDV-L from infected onion to both onion and garlic at the rate of 17% and 30%, respectively (Table 5). These results clearly indicate that the OYDV-S was not transmitted to garlic by aphids when it was not coinfected with LYSV. In contrast, OYDV-L was readily transmitted to both garlic and onion by aphids.

It is quite likely that HC-Pro of LYSV can function *in trans* as a bridge between both LYSV and OYDV to bind to stylet receptors. Several studies have supported the role of potyviral HC-Pro as the "bridge" between the CP and aphid stylet (Pirone and Blanc 1996). It has been previously reported that potato virus Y can partially complement the aphid transmissibility of a and tobacco etch virus isolate with a truncated HC-Pro (Dolja et al. 1993).

To confirm the above hypothesis of the molecular interaction in which LYSV HC-Pro binds to OYDV CP, we attempted to detect the binding between the two proteins by the pull-down assay with His-affinity gel. As shown in Fig. 5, the OYDV CP was detected in the pull-down fraction of HC-Pro. This suggest that two proteins may interact and bind to each other. To detect the direct binding of both proteins, a Far-Western dot blot assay was performed using purified HC-Pro and CP. The results showed that HC-Pro and CP bound to each other in a reciprocal combination (Fig. 6). By using several deletion mutants, the binding domain of HC-Pro, was narrowed down to the region between 150-233 amino acid residue. With these data, we presumed that the two proteins were likely to bind. Anyway, additional experiments are needed to fully exploit the bonding mechanism.

CONCLUSION

The short-type HC-Pro has lost aphid transmissibility. In addition, the short-type HC-Pro has reduced its RSS activity; hence, OYDV-S induces mild symptoms in garlic. Production of mild symptoms may have helped the OYDV-S to infect and spread unnoticedly in Japanese garlic. Therefore, the mutation in the HC-Pro gene has given OYDV-S an advantage to survive under the man-made selection pressure in the Japanese garlic fields. The loss of aphid transmissibility due the mutation has been compensated by the symbiotic interaction with LYSV. On the other hand, OYDV-L produces more severe symptoms and is thus prone to be noticed and eventually culled by farmers, making the OYDV-L strain rarer in Hokkaido. The mild symptoms induced by the OYDV-S isolates may have a certain competitive advantage under this man-made selection pressure and still be horizontally transmitted with the help of LYSV.

Chapter 2: Evolution of a quadripartite symbiosis driven by a satellite RNA to promote aphid transmission

INTRODUCTION

Plant viruses are obligate parasites that use their host plant cells to reproduce themselves. Consequently, these viruses need to spread to new hosts, and many plant viruses depend on insect vectors in this process. Viruses are also associated with subviral non-cording RNA molecules such as satellite RNAs (satRNAs) which can modify the viral accumulation levels and the symptoms caused by the helper virus (Shimura et al. 2011). Since viruses are differentially transmitted by insect vectors, any change in virus-vector interactions would affect the natural selection of virus population. Thus, it is important to understand the dynamics and evolution of satRNAs and helper viruses in the nature.

Cucumber mosaic virus and its satellite virus; Y-sat modulates host gene expression

Cucumber mosaic virus (CMV) is one of the most successful viral pathogen as it can infect nearly 1200 plant species (Ziebell et al. 2011). Y satellite RNA (Y-sat) is one of the satRNAs which depends on CMV for its replication and encapsidation (Shimura et al. 2011). Presence of Y-sat in CMV-infected *Nicotiana* plants changes the normal mosaic symptoms into bright yellowing of leaves (Figure 8). Y-sat specifically down-regulates the *ChlI* mRNA, impairing the chlorophyll biosynthesis in *Nicotiana* plants (Shimura et al. 2011).

Figure 8 Presence of Y-sat in CMV-infected *Nicotiana* plants changes the normal mosaic symptoms into bright yellow. From left to right, healthy, CMV-infected and [CMV+Y-sat]-infected *N. tabacum* plants.

Coevolution of a quadripartite interaction between plant, virus, vector and satellite virus

Y-sat seems not to compete with other similar-size satRNAs (Masuta et al. 1990), suggesting that Y-sat may have a different strategy for its survival in the nature. CMV with Y-sat are transmitted mainly by aphid species *Aphis gossipii* (Escriu et al. 2000) and *Myzus persicae* (green peach aphid) while the latter is found in many countries and has a wide host rang (Ziebell et al. 2011). CMV is non-persistently transmitted and the primary determinant of aphid transmissibility is the viral coat protein (Escriu et al. 2000; López-Moya 2002). CMV particles bind loosely to the receptors in the acrostyle of aphid, but the exact receptor molecules in the aphid stylet is unknown (Webster et al. 2018). Nevertheless, it has been believed that the transmission of CMV positively correlated with the accumulation of CMV in the host tissue. Presence of satRNAs reduces the accumulation of the helper virus which negatively affects the transmission of the helper virus (Escriu et al. 2000). If the satRNA greatly reduce the helper virus accumulation levels, the frequency of Y-sat transmission to new hosts is negatively affected and the satRNA should disappear with time (Escriu et al. 2000). Therefore, it is anticipated that both the satRNA and helper virus must have coevolved to have a synergistic interaction so that both of them can survive.

Recent works has advanced the knowledge of the coevolution of viruses, hosts and vectors. Somehow we still don't know how satRNAs have shaped the coevolution of the virus, host and vector, modulating interactions among four trophic levels (Wang et al. 2017; Carr et al. 2018).

METERIALS AND METHODS

Plant material maintenance

Tobacco (*Nicotiana tabacum* L. cv BY4 and *N. benthamiana*) seedlings were maintained in a plant growth room at 24°C under artificial light 16L:8D hrs.

Insect stocks

Colonies of *M. persicae* (Sulzer) were maintained on *Brassica rapa* plants at 24°C under artificial light with photoperiod of 16hrs. Separately, *M. persicae were* maintained on broad bean (*Vicia faba*) seedlings, at two conditions i.e., at high densities (>20 individuals/seedling) or at low densities (2 individuals/seedling).

Virus and satellite virus inoculation

CMV strain O (CMV-O) was used as the helper virus for Y-sat and maintained on tobacco plants by rub-inoculation.

Life history study of *M. persicare*

Started from a single adult aphid placed on a *V. faba,* aphids were grown in a 50 ml tube under the constant conditions of 24ºC and 16:8 day and night cycle. Viviparous daughters and granddaughters of the above individuals were used for the experiments.

All red and green aphids were separated from a 3-week-old colony. Twenty green and 17 red nymphs were collected and reared on *V. faba.* These aphids were placed on seedlings and observed daily until reproduction maturity.

Twenty-five one-day-old aphids were individually reared to observe the morphology and the life history of each aphid. Selected individuals were photographed every day using Dino-eye (AM321) or Ricoh digital camera (WG-4). Each aphid was observed daily and days for each moulting was counted by observing the exuviae.

Detection of *M. persicae* densovirus (MpDNV) in aphids

DNA was extracted using five alate and five apterous aphids from the N3 instar from the colony maintained in the laboratory, using the nucleic acid extraction buffer followed by standard phenol chlorophome extraction. Presence of MpDNV was tested using a primer pair of (5′TGACAATGGGTATATTCATTGACCT3′ and 5′ATCGTGCGTCAAAAGAAACCCT3′) in the aphid's DNA.

Pairwise aphid attraction bioassays for colour

M. persicae aphids maintained on *V. faba* were used for the bioassay. For each pair-wised bioassay, two *N. tabacum* plants were placed in a 35x15x20cm glass box at 30cm apart as shown in fig. 9. Aphids were starved for 3hrs and 20-30 starved winged aphids were used. During a period of two hours, at every ten minutes, the number of aphids present on each plant was recorded. Each experiment was replicated for four times by changing the orientation of the plants from left to right and vice versa.

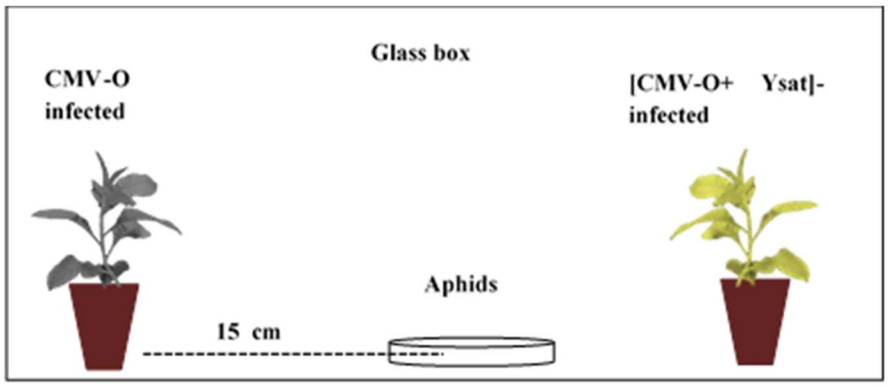

Figure 9 Experimental setup for the pairwise aphid attraction bioassay.

Y-tube bioassay for attraction to VOCs

For the Y-tube bioassay, *N. tabacum* plants, infected with CMV-O, CMV-O+Y-sat and healthy were used. Plants of the same age and size were selected and around 50 *M. persicae* aphids were used for the test. The arrangement of the experiment is explained in the Figure 10. Once the aphid walked forward the selected arm it was considered as the aphid's choice. Each aphid was given 2 minutes testing period. The plants were interchanged after every 10 tests.

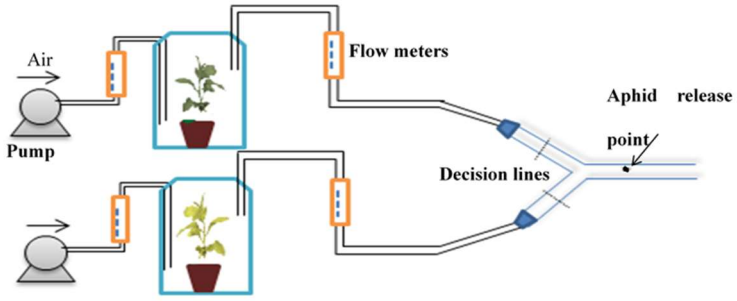

Figure 10 Experimental setup for the Y-tube aphids attraction bioassay.

RT-q-PCR for CMV in infected plants

RT-q-PCR was performed to quantitate CMV in infected plants. Total RNA from plant tissues were extracted using the conventional phenol/chloroform method and reverse-transcribed using Takara Perfect Real Time, PrimeScript™ RT reagent Kit. Quantitative PCR was performed with StepOnePlus™ Real-Time PCR System, using SYBR Green Master Mix (Appliedbiosystems). 18S was used as the internal control (the primer pair: $^{5'}$GCAAGACCGAAACTCAAGG$^{3'}$ and $^{5'}$TGTTCATATGTCAAGGGCTGG$^{3'}$). For CMV, a primer pair of $^{5'}$GTTGACGTCGAGCACCAACGC$^{3'}$ and $^{5'}$TGGTCTCCTTTTGGAGGCCC$^{3'}$ were used.

RT-q-PCR for CMV in individual aphid

Total RNA from *M. persicae* was extracted using Trizol (Invitrogen) following the manufactures protocol. Total RNA was recovered by centrifugation and dissolved in 6µl of RNase free water and reverse-transcribed using AMV reverse transcriptase. Quantitative PCR was performed with

StepOnePlus™ Real-Time PCR System, using SYBR Green Master Mix (Appliedbiosystems). Partial ribosomal protein S3 (Rps3) of aphid was used as an internal control (the primer pair: $^{5'}$CGAGCTGCTCCATCTCGTA$^{3'}$ and $^{5'}$CCCACTTTCCATGATGAATCTCA$^{3'}$). For CMV, a primer pair of $^{5'}$GTTGACGTCGAGCACCAACGC$^{3'}$ and $^{5'}$TGGTCTCCTTTTGGAGGCCC$^{3'}$ were used.

RT-q-PCR for *Apns1* in aphid

For quantification of the *Apns1* gene in aphids, total RNA was extracted separately from alate and apterous morphs using 10-15 3rd instar (N3) and from single aphids at early adult (A(1)) stage. Extraction of RNA was done as described above. The β-tubulin gene of aphid was used as internal control (the primer pair: 5'CCATCTAGTGTCGCTGACCA3' and 5'GTTCTTGGCGTCGAACATTT3'). For *Apns1,* a primer pair of *5*'CCGGCGCAATGACGGAACTGA3' and 5'CCATGGCACCAACGGCGATGA3' were used.

RT-q-PCR for *ABCG4* in aphid

For quantification of the *ABCG4* gene in aphids, total RNA was extracted separately from alate morphs of 3rd instar and from single aphids at A(1) stage. Extraction of RNA was done as described above. The β-tubulin gene of aphid was used as an internal control (the primer pair: 5'CCATCTAGTGTCGCTGACCA3' and 5'GTTCTTGGCGTCGAACATTT3'). For *ABCG4,* a primer pair of 5'AACTGCCCTGTCCCATCTAT3' and 5'GGTGTGTCATTGATGGCTAG3' were used.

Transmission of CMV from CMV-O-infected and [CMV-O+Y-sat]-infected plants

Apterous *M. persicae* aphids staved for 3hr were subjected to a 2-5min acquisition access period on CMV-O- and [CMV-O + Y-sat]-infected *N. tabacum*. Aphids were observed whether they probe on the leaf, and 10 aphids were collected, transferred to each healthy *N. tabacum* plant using a fine dry paintbrush. The aphids were then killed using a pesticide after one day. Infection

was confirmed by the visual symptoms after 1-2weeks. Ten test plants per treatment and two replications were used.

Intrinsic rate of increase of aphids grown on CMV-O-infected, [CMV-O+Y-sat]-infected and healthy plants

One aphid per clip-cage, one cage per plant and three plants per treatment were used. Aphid, less than one day old was confined in a clip cage for seven days. The intrinsic rate of increase (r_m) for each aphid was calculated as proposed by Wyatt and White (1977).

Jasmonic acid levels in CMV-O-infected, [CMV-O+Y-sat]-infected and healthy plants

The levels of Jasmonic acid were measured from the 45 dpi leaf tissues of healthy, CMV-O- and [CMV-O+Y-sat]-infected *N. tabacum* plants. Leaf samples are immediately weighed, frozen in liquid nitrogen and stored at -80°C. Ultra-performance liquid chromatography-tandem mass spectrometry was conducted to measure the level of jasmonic acid in the plant tissue.

Level of glucose and sucrose in plant tissues CMV-O-infected, [CMV-O+Y-sat]-infected, CMV-L-infected and [CMV-L+Y-sat]-infected and healthy tobacco plants

Using three plants at the 45dpi stage, the levels of sugars were measured from healthy and infected *N. tabacum* plants. Leaf tissue were prepared as described by Fredeen et al. 1989. Sucrose and glucose levels of the sample were analysed by enzymatic techniques (Boehringer Mannheim Enzymatic BioAnalysis for sucrose, d-glucose and d-fructose determination, R-Biopharm AG) following manufacturers protocol.

Photosynthesis levels of CMV-O-infected, [CMV-O+Y-sat]-infected, CMV-L-infected and [CMV-L+Y-sat]-infected and healthy tobacco plants

Photosynthesis rate at each light condition was measured using miniPPM-200 following the manufacturer's instructions. Photosynthesis was measured at 15dpi and 30dpi using three plants per treatment and two readings per plant. Plants were first adapted to dark conditions by keeping them in dark overnight. Initially F_{ref} value was fixed by doing a pre-test under dark condition

(PAR=0 µmol/m2/s). First reading was taken at the dark condition (PAR=0 µmol/m2/s), and the light condition was increased step by step while giving 10-15 min adaptation period before the measurements.

Stomata conductance CMV-O-infected, [CMV-O+Y-sat]-infected, CMV-L-infected and [CMV-L+Y-sat]-infected and healthy tobacco plants

Stomata conductance at each light condition was measured using Leaf Porometer, modal SC-1, Decagon Devices, Inc. using the manufactures instructions. Measurements were taken from the third or fourth leaf of each plant in each treatment from three plants per treatment. All the measurements were taken during 11.00 am-3.00 pm at 24-27°C.

Number of alate and apterous aphids on Y-sat-transgenic expressing Y-sat dsRNA and wild *N. benthamiana* plants

One to two day-old, twenty *M. persicae*, which were reared under low densities, were introduced to the Y-sat inverted repeat expressing transgenic and wild type *N. benthamiana* plants and reared at the same conditions. The number of alate and apterous aphids was counted after 28 days after introduction.

Number of alate and apterous aphids on healthy, CMV-O-infected and [CMV-O+Y-sat]-infected *N. tabacum* plants

One to two day-old, twenty *M. persicae*, which were reared under low densities, were introduced to, healthy, CMV-O- and [CMV-O+Y-sat]-infected *N. tabacum* plants and reared at the same conditions. The number of alate and apterous aphids were counted on the 28th and 35th day.

Number of alate and apterous aphids on *N. benthamiana* leaves expressing Y-sat dsRNA, plus-sense Y-sat or negative-sense Y-sat.

The pBE2113 vectors were constructed by inserting the above sequences in between the Xbal and Sacl sites and inserted to *A. tumefaciens* (KYRT1) by the conventional freeze-thaw method. Then cultured on YEP medium followed by the incubation for 48hrs. The culture was precipitated,

harvested and re-suspended in the agrobacterium resuspension buffer, and the optical density was adjusted to 0.6 at O.D.600. After 2-3hrs, *N. benthamiana* leaves were infiltrated with the inoculum. The GUS gene was used as the control.

Thirty-50 *M. persicae*, which were reared under low densities were introduced to the *N. benthamiana* leaves at 1 dpi, and reared at the same conditions. The number of alate and apterous morphs was counted 4 days after introduction.

Wing induction study on transgenic *N. benthamiana* expressing Y-sat dsRNA, plus-sense Y-sat, negative-sense Y-sat and wild-type plants

Similarly, 30 *M. persicae*, were introduced to the transgenic *N. benthamiana* and wild-type plants and reared at the same conditions. The number of alate and apterous aphids was counted 5 days after introduction.

Effect of Y-sat dsRNA on aphid wing formation by artificial feeding

Artificial diet previously developed for *M. persicae* (Mittler and Dadd 1962) was used for the basal diet. Two hundred micro litters of the artificial diet were pipetted on the membrane and around 7µl of dsRNA (dsRNA of Y-sat or LYSV) or dH_20 was mixed by pipetting (final concentration 100 ng/µl). The diet was then covered with another piece of Parafilm that was stretched 4 times.

Two day-old 25-30 *M. persicae*, at low densities were placed in the lid using brush. Feeding apparatus was conducted as explained by Paula et al. (2016). The number of alate and apterous morphs was counted 4 days after introduction.

sRNA data analysis.

Aphids were reared for several generations on healthy *N. tabacum*, CMV-O-infected *N. tabacum*, [CMV-O+Y-sat]-infected *N. tabacum* and Y-sat IR transgenic *N. benthamiana* and wild-type *N. benthamiana* plants. Total RNA was extracted from the apterous and alate morphs of the N3 instar

and subjected to NGS and the size specific distribution of sRNA was analysed by SAMtools, bam2fastq and C.

RNA dot blot hybridization

Single stranded small RNAs of Y-sat, AcABCG4, and miR171b were dotted onto Amersham Hybond-N+ membrane (GE Healthcare) with a serial dilution (10, 4, 1, 0.4 pmol). The membrane was soaked with 20X SSC buffer (3M NaCl, 0.3M sodium citrate), and the RNAs are cross-linked to membrane using UV Crosslinker CX-2000 (UVP). The dotted RNAs were probed with 50 nM Digoxigenin (DIG)-tagged miR-9b in hybridization buffer (50% formamide, 0.63 M NaCl, 60 mM sodium citrate, 20 mM maleic acid, 2% Blocking reagent (Roche), 7% SDS, 0.6% N-lauryl sarcosine, 25 mM Na2HPO4) at 40℃ overnight. After washing with the washing buffer (0.3 M NaCl, 30 mM sodium citrate, 0.1% SDS) and followed blocking in blocking buffer (0.1 M maleic acid, 0.15 M NaCl, 1% Blocking reagent) for 1 h, the membrane was treated with Anti-Digoxigenin-AP, Fab fragments (Sigma-Aldrich) in DIG reaction buffer (0.1 M maleic acid, 0.15 M NaCl, 1% Blocking reagent, 0.3% tween 20) for 0.5 h. After washing with DIG washing buffer (0.1 M maleic acid, 0.15 M NaCl and 0.3% tween 20), the DIG was detected by alkaline phosphatase reaction in LAS4000 (Fujifilm). Synthetic sRNA used are as follow.

Y-sat: ACGAUGGUGGGAGUCACCCAAGGGG

AcABCG4: AAUUGGAAAAGGAACCAAAGA

miR171b: UGAUUGAGCCGCGCCAAUAUC

miR-9b probe: UCUUUGGUACUUUAGCUGUAG

RESULTS

Life history study of *M. persicare*

Table 6 Number of red and green aphids in the 3 week-old colony

Body colour	Number
Green	98 (including N1 and N2)
Red	17

N-Nymph

Table 7 Fate of green and red nymphs after 5-6 days observation

Body colour	Number	Fate	
		Apterous	Alates
Green	20	18	0
Red	17	0	17

Green and red aphids from a colony grown for 3 weeks from an individual aphid were counted and separated. There was a total of 115 individual aphids of varying ages, out of them, 17 red nymphs were identified (Table 6). Randomly-selected 20 green nymphs and the 17 red nymphs were separately reared. Out of twenty, 18 green individuals were grown into apterous female. Two individuals died at an early stage. All 17 red aphids were grown into alate female (Table 7).

Fate of the green and red nymphs (N- Nymph)

Day 1/ N1

Day 2/ N2

Day 3 / N3

Green

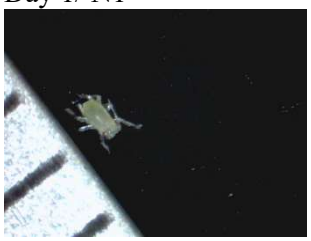

N3

Red

Day 4 / N3

Day 5/ N4

Day 6 / N4

Green

N3

N4

N4

Red

Figure 11 Life history data of *M. persicare* with respect to wing formation

Table 8 Number of nymphal stages pass to become adult

No	Days old												Body colour	Fate
	0	1	2	3	4	5	6	7	8	9	10	11		
1	N1	N2	N3	N3	N3	N4	A(1)	A(1)	A(1)	A(2)			G	Ap
2	N1	N2	N3	N3	N4	N4	A(1)	A(1)	A(2)				G	Ap
3	N1	N2	N2	N3	N3	N4	A(1)	A(1)	A(1)	A(2)			G	Ap
4	N1	N2	N3	N3	N3	N4	A(1)	A(1)	A(2)				G	Ap
5	N1	N2	N3	N3	N4	N4	A(1)	A(1)	A(1)	A(1)	A(2)		G	Ap
6	N1	N2	N3	N3	N3	N4	A(1)	A(1)	A(1)	A(2)			G	Ap
7	N1	N2	N3	D										
8	N1	N2	N3	N3	N3	N4	A(1)	A(1)	A(1)	A(2)			G	Ap
9	N1	N2	N3	N3	N4	A(1)	A(1)	A(1)	A(2)				G	Ap
10	N1	N2	N3	N3	N4	N4	A(1)	A(1)	A(1)	A(2)			G	Ap
11	N1	N2	N3	N3	N3	N4	D						G	
12	N1	N2	N2	N3	N3	N4	A(1)	A(1)	A(2)				G	Ap
13	N1	N2	N3	N3	N3	N4	N4	A(1)	A(2)				G	Ap
14	N1	N2	D											
15	N1	N2	N3	N3	N4	N4	A(1)	A(1)	A(1)	A(2)			G	Ap
16	N1	N2	N3	N3	N4	N4	A(1)	A(1)	A(1)	A(2)	D		R	
17	N1	N2	D											
18	N1	N2	N3	N3	N3	N4	A(1)	A(1)	A(1)	A(2)			G	Ap
19	N1	N2	N3	N3	N4	N4	A(1)	A(1)	A(1)	A(1)	A(2)		G	Ap
20	N1	N2	N3	N3	N4	A(1)	A(1)	A(1)	A(1)	A(2)			G	Ap
21	N1	N2	N2	N3	N3	N4	A(1)	A(1)	A(1)	A(2)			G	Ap
22	N1	N2	N3	N3	N3	N4	A(1)	A(1)	A(2)				G	Ap
23	N1	N2	N3	N3	N4	N4	A(1)	A(1)	A(2)				G	Ap
24	N1	N2	N3	N3	N4	N4	N4	N4	A(1)	A(1)	A(2) &(3)	A (4)	R	Al
25	N1	N2	N3	N3	N4	N4	A(1)	A(1)	A(2)				G	Ap

N-Nymph, A-Adult, G-Green, R-Red, Ap-Apterous, Al-Alate

The green and red morphs passed four nymphal instars to become adults. In red morph life cycle, the wing buds become visible at the early adult stage (A(1)) stage and in the successive growth, the wing bud grew further and became white in colour. During the A(3), the wings were further extended but remained unexpanded. After the final moult, the aphid with functioning wings could be seen (A(4)), and they became blackish, but some red-fading was observed in the body (Fig. 11 and Table 8).

Detection of *M. persicae* densovirus (MpDNV) in aphids

a b

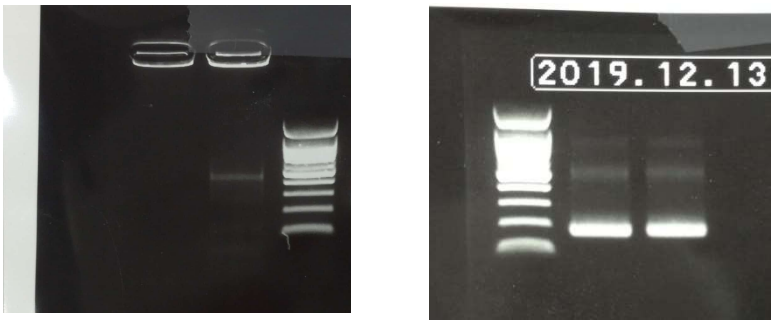

Figure 12 Detection of *M. persicae* densovirus (MpDNV) in aphids. a. specific primers for MpDNV were used to detect the virus and virus was not detected. b. β-tubulin of aphid was detected in same samples

MpDNV was not detected in the *M. persicare* colony maintained. The β-tubulin gene of aphid was used as a control (Fig. 12).

Pairwise aphid attraction bioassays for colour

Table 9 Percentage of aphids attracted to CMV-O-infected and [CMV+Y-sat]-infected plants

Time after release (min)	R1 n-20		R2 n-28		R3 n-30		R4 n-33	
	% CMV+Y-sat	% CMV	% CMV+Y-sat	% CMV	% CMV+Y-sat	% CMV	% CMV+Y-sat	% CMV
60	26.67	13.33	27.27	9.09	31.58	15.79	25.00	10.00
120	20.00	0.00	36.36	9.09	26.32	10.53	31.58	21.05

Table 10 Percentage of aphids attracted to healthy and [CMV+Y-sat]-infected plants

Time after release (min)	R1 n-30		R2 n-37		R3 n-46		R4 n-37	
	% CMV+Y-sat	% Healthy	% CMV+Y-sat	% Healthy	% CMV+Y-sat	% Healthy	% CMV+Y-sat	% Healthy
60	16.67	0.00	20.68	6.69	13.16	7.89	31.43	14.29
120	18.75	12.50	20.68	10.3	18.42	10.53	29.41	17.65

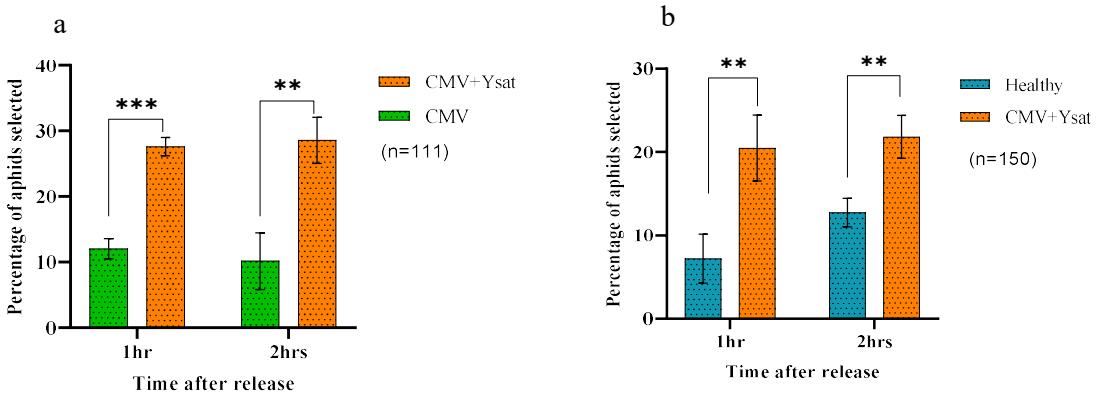

Figure 13 Percentage of Aphids selected CMV-O-infected, [CMV-O+Y-sat]-infected or healthy plants after 1 hr and 2 hrs. Data are mean percentages of four replicates. **a)** [CMV-O+Y-sat]-infected plants which showed bright yellow symptoms attracted significantly more aphids than CMV-O- infected N. tabacum plants. A total of 111 aphids were used and after 1 hr [CMV-O+Y-sat]-infected and CMV-infected plant attracted 27.63% and 12.05% aphids respectively (P= 0.0007) while after 2 hrs 28.57% and 10.17% respectively. **b)** When compared with Healthy and [CMV-O+Y-sat]-infected plants a significantly higher number of aphids got attracted to [CMV-O+Y-sat]-infected plants after 1 hr ([CMV-O+Y-sat]-, 20.31%; healthy, 6.38% (P= 0.032)) and 2 hrs ([CMV-O+Y-sat]-, 20.35%; healthy, 13.87% (P= 0.114)). A total of 150 aphids were used. *** P<0.001, **P<0.05.

The proportion of aphids attracted to [CMV-O-+Y-sat]-infected plants were significantly higher at 1 hr and 2 hrs observation points (1 hr: p=0.0007; 2 hrs: p=0.021) (Fig 13a and Table 9). When tested against healthy and [CMV-O-+Y-sat]-infected tobacco plants, the number of aphids selected on the Y-sat infected plants were significantly higher (1 hr: p=0.032; 2 hrs: p=0.0026) (Fig 13b and Table 10).

Y-tube bioassay for attraction to VOCs

Table 11 Number of aphids attracted to each *N. benthamiana* plant in the Y-tube olfactory bioassay

No choice	[CMV-O+Y-sat]	CMV	No choice	[CMV-O+Y-sat]	Healthy	No choice	CMV-O	Healthy
18	7	9	23	8	6	22	8	9

Table 12 Number of aphids attracted to each *N. tabacum* plant in the Y-tube olfactory bioassay

No choice	[CMV-O+Y-sat]	CMV	No choice	[CMV-O+Y-sat]	Healthy	No choice	CMV-O	Healthy
28	10	11	30	8	6	28	5	7

a

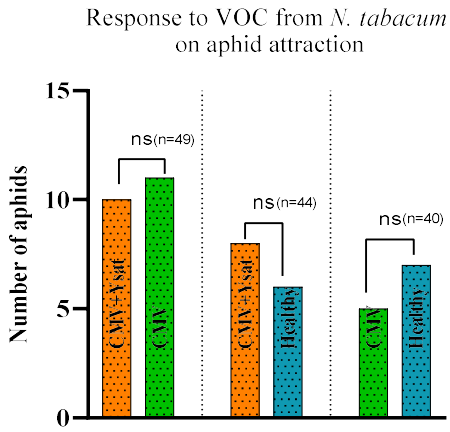

b

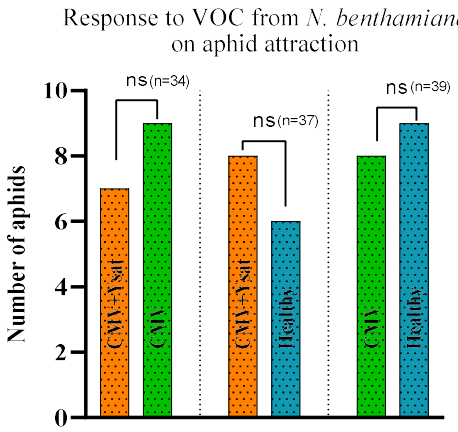

Figure 14 Response to volatile compounds from infected tobacco on aphid attraction using the Y-tube experiment. **a)** 34 aphids were allowed to select [CMV-O+Y-sat]-infected or CMV-O-infected plants and aphids did not show a significant difference among aphids' choice (P=0.8). Thirty-seven individual aphids were allowed to select [CMV-O+Y-sat]-infected or healthy plants and did not show any tendency to select one over the other (P=0.79). In the same way 39 aphids were allowed to select healthy plant vs CMV-O-infected plant, did not show any tendency to select one over the other (P=0.99). (Tow-tailed Fisher's Exact Test). **b)** *N. tabacum* was used to test the aphid attraction. Forty-four individual aphids were allowed to select either [CMV-O+Y-

sat]-infected or CMV-O-infected plants, and aphids did not show tendency to select [CMV-O+Y-sat]-infected plants vs CMV-O-infected plants (P=1.0). In the same way, 49 aphids were allowed to select [CMV-O+Y-sat]-infected or healthy plants also did not show any tendency to select one over the other (P=0.79). Thirty-five individual aphids were allowed to select healthy plant vs CMV-O-infected plant where similarly there was no significant difference among aphids' choice (P=0.77). Experiment was carried out under the normal illumination using 15-18 days post inoculation and with plants of the same size. (ns = not significant)

In the olfactory bioassay with CMV-O-infected and [CMV-O-+Y-sat]-infected *N. benthamiana* plants, it was evident that there was no significant difference over the choice (Fisher's exact test, p=0.80) neither when [CMV-O-+Y-sat]-infected vs healthy *N. benthamiana* plants were used (Fisher's exact test, p=0.79) nor when CMV-O-infected vs healthy *N. benthamiana* plants were used (Fisher's exact test, p=0.99) (Fig. 14a and Table 11).

In the olfactory bioassay using CMV-O-infected and [CMV-O-+Y-sat]-infected *N. tabacum* plants, it was evident that there was no significant difference over the choice (Fisher's exact test, p=1.0) neither when [CMV-O-+Y-sat]-infected vs healthy *N. tabacum* plants were used (Fisher's exact test, p=0.79) nor when CMV-O- infected vs healthy *N. tabacum* plants were used (Fisher's exact test, p=0.77) (Fig. 14b and Table 12).

Photosynthesis levels of CMV-O-infected, [CMV-O+Y-sat]-infected, CMV-L-infected, [CMV-L+Y-sat]-infected and healthy plants

Table 13 Photosynthesis rates of *N. tabacum* healthy, CMV-O-infected and [CMV-O+Y-sat]-infected plants at 30 dpi

PAR value	Healthy				CMV-O				CMV-O+Y-sat			
0	0	0	0	0	0	0	0	0	0	0	0	0
30	27	19	20	22	17	19	22	20	14	20	19	17
50	29	29	33	32	27	31	32	29	25	32	27	33
60	38	43	34	41	35	37	35	38	30	31	31	33
75	47	43	46	47	41	42	43	43	42	37	42	45
120	76	71	64	70	71	67	69	63	70	68	71	66
740	226	145	285	191	222	186	131	104	171	217	185	225
1100	230	236	222	238	198	220	258	225	187	252	240	234

Unit- µmol/m2/s

Table 14 Photosynthesis rates of *N. tabacum* healthy, CMV-L-infected and [CMV-L+Y-sat]-infected plants at 30 dpi

PAR value	Healthy			CMV-L			CMV-L+Y-sat		
	0	0	0	0	0	0	0	0	0
30	19	20	25	25	18	21	17	18	14
50	35	44	34	32	34	31	28	29	33
60	45	35	33	33	34	31	28	29	33
75	46	49	54	48	46	48	45	34	33
120	73	75	69	69	66	63	67	62	68
400	91	95	81	84	71	81	80	72	85
600	125	138	130	115	125	123	108	120	105
1200	205	253	261	167	171	257	184	172	252

Unit- µmol/m2/s

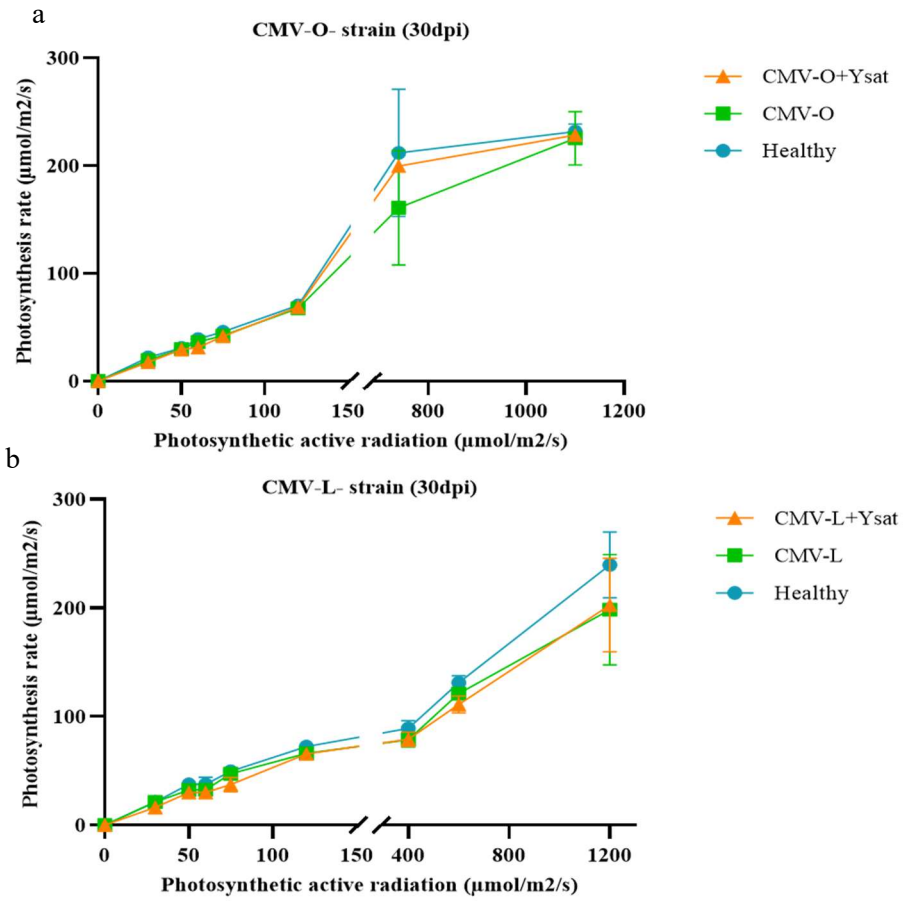

Figure 15 Photosynthesis rates measured 30 dpi in the plants infected with CMV and [CMV+Y-sat] and healthy. Two strains of CMV were used: CMV-O and CMV-L. **a)** Photosynthesis rate of CMV-O-infected, [CMV-O+Y-sat]-infected and healthy *N. tabacum* plants with increasing photosynthetic active radiation levels. At 30 dpi, low light to mid light conditions (at 30-120 µmol/m2/s photosynthetic active radiation (PAR)) the photosynthetic rate of healthy, CMV-O-infected and [CMV-O-+Y-sat]-infected plants did not show any significant difference (CMV-O: 30 dpi:120 µmol/m2/s:Tukey's test, p=0.591). In general, the photosynthetic efficiency was reduced in Y-sat-infected plants at higher light intensities (clear sunny environment, at 1100-1200 µmol/m2/s PAR) nevertheless did not show a significant difference among the treatments (CMV-O: 30 dpi:1200 µmol/m2/s:Tukey's test, p= 0.924). Data are means $\pm$ SE (n=4). **b)** Photosynthesis rate of CMV-L-infected, [CMV-L+Y-sat]-infected and healthy *N. tabacum* plants with increasing photosynthetic active radiation levels. No significant difference in photosynthetic rate were observed (CMV-L: 30 dpi:120 µmol/m2/s:Tukey's test, p=0.066; CMV-L: 30 dpi:1200 µmol/m2/s: Tukey's test, p= 0.467) Data are means $\pm$ SE (n=3).

Table 15 Photosynthesis rate of *N. tabacum* healthy, CMV-O-infected and [CMV-O+Y-sat]-infected plants at 15 dpi

PAR value	Healthy				CMV-O				CMV-O+Y-sat			
0	0	0	0	0	0	0	0	0	0	0	0	0
30	25	25	23	24	22	20	23	19	23	20	17	17
50	36	33	34	28	27	30	28	24	22	30	27	27
60	42	39	39	45	36	34	32	36	34	32	34	31
75	49	54	52	53	54	49	47	47	45	44	41	48
120	82	79	71	78	70	52	59	63	58	63	46	52
650	155	114	176	180	119	180	146	157	115	114	176	135
1200	265	117	234	211	261	200	132	196	167	166	161	143

Unit- µmol/m2/s

Table 16 Photosynthesis rate of *N. tabacum* healthy, CMV-L-infected and [CMV-L+Y-sat]-infected plants at 15 dpi

PAR value	Healthy			CMV-L			CMV-L+Y-sat		
0	0	0	0	0	0	0	0	0	0
30	18	22	23	18	20	24	25	17	22
50	39	27	33	23	30	28	37	32	33
60	36	42	36	37	38	35	34	32	33
75	54	48	42	40	45	48	40	40	44
120	60	61	63	54	65	64	63	56	59
600	174	145	141	146	138	145	129	71	113
1100	173	141	143	150	144	109	92	85	113

Unit- µmol/m2/s

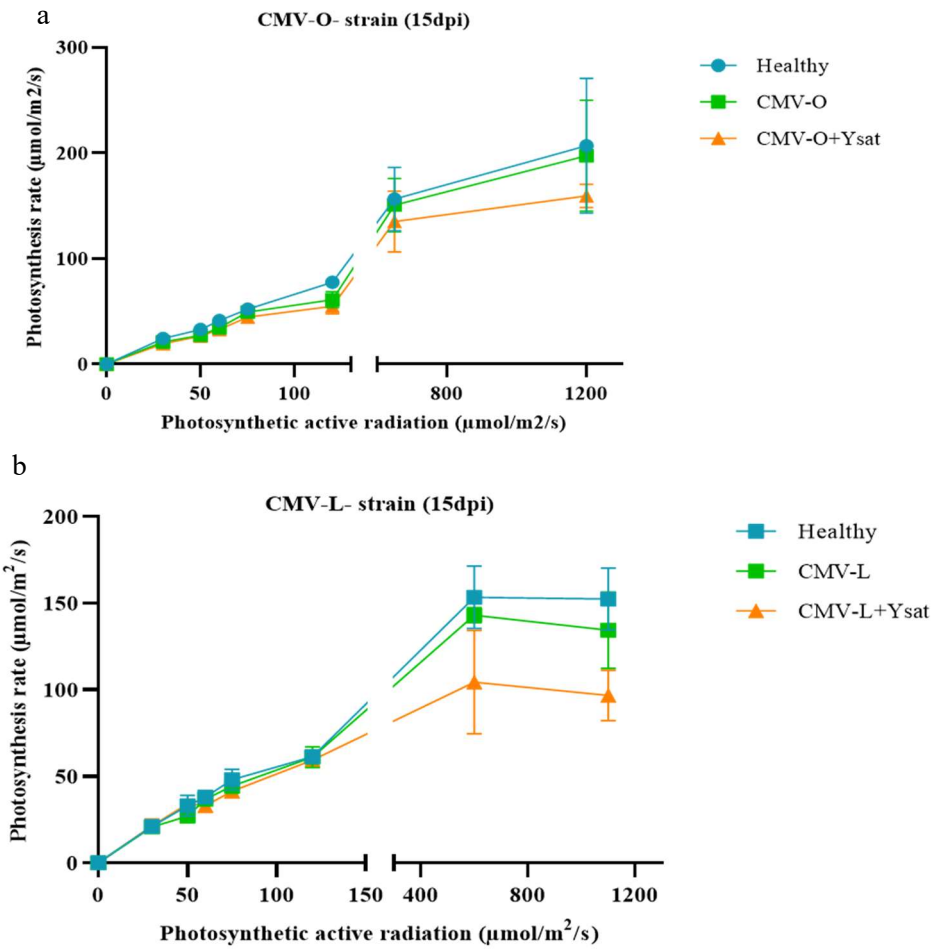

Figure 16 Photosynthesis rates measured 15 dpi using CMV-infected and [CMV+Y-sat]-infected and healthy plants. Two strains of CMV were used: CMV-O and CMV-L. **a)** Photosynthesis rates of CMV-O-infected, [CMV-O+Y-sat]-infected and healthy *N. tabacum* plants with increasing photosynthetic active radiation levels. Reduction of photosynthesis rate at mid PAR was significant in the [CMV-O+Y-sat]-infected plants (CMV-O:15 dpi:120 µmol/m2/s:Tukey's test, p=0.003 but not in higher PAR levels (CMV-O:15 dpi:1200 µmol/m2/s:Tukey's test p= 0.378). Data are means ± SE (n=4). **b)** Photosynthesis rate of CMV-L-infected, [CMV-L+Y-sat]-infected and healthy *N. tabacum* plants with increasing photosynthetic active radiation levels. Reduction in photosynthesis rate at higher PAR was significant in the [CMV-L+Y-sat]-infected plants (CMV-L:15 dpi:1100 µmol/m2/s:Tukey's test, p= 0.026) but not at mid PAR levels (CMV-L:15 dpi:120 µmol/m2/s:Tukey's test, p=0.824). Data are mean ± SE (n=3).

Photosynthesis rates were measured at 30 dpi in the CMV-infected, [CMV+Y-sat]-infected and healthy plants. Two strains of CMV (CMV-O and CMV-L) were used. We measured the

photosynthesis rates of CMV-O-infected, [CMV-O+Y-sat]-infected and healthy *N. tabacum* plants with increasing photosynthetic active radiation levels (Fig. 15a and Table 13). At 30 dpi, the low light to mid light conditions (at 30-120 µmol/m2/s photosynthetic active radiation (PAR), the photosynthetic rate of healthy, CMV-O-infected and [CMV-O-+Y-sat]-infected plants did not show a significant difference (CMV-O:30 dpi:120 µmol/m2/s:Tukey's test, p=0.591). In general, photosynthetic efficiency was reduced in the Y-sat infected plants at higher light intensities (clear sunny environment, at 1100-1200 µmol/m2/s PAR) nevertheless did not show any significant difference among the treatments (CMV-O:30 dpi:1200 µmol/m2/s:Tukey's test, p= 0.924) Data are means $\pm$ SE (n=4). We measured the photosynthesis rates of CMV-L-infected and [CMV-L+Y-sat]-infected and healthy *N. tabacum* plants with increasing photosynthetic active radiation levels (Fig. 15b and Table 14). No significant difference in photosynthetic rate were observed (CMV-L:30 dpi:120 µmol/m2/s:Tukey's test, p=0.066; CMV-L:30 dpi:1200 µmol/m2/s:Tukey's test, p= 0.467).

We measured the photosynthesis rates 15 dpi in the CMV-infected and [CMV+Y-sat]-infected and healthy plants. Two strains of CMV were used: CMV-O and CMV-L. We measured the photosynthesis rates in the CMV-O-infected and [CMV-O+Y-sat]-infected and healthy *N. tabacum* with increasing photosynthetic active radiation levels (Fig. 16a and Table 15). Reduction in photosynthesis rate at mid PAR was significant in the [CMV-O+Y-sat]-infected plants (CMV-O:15 dpi:120 µmol/m2/s: Tukey's test, p=0.003 but not in higher PAR levels (CMV-O:15 dpi:1200 µmol/m2/s: Tukey's test p= 0.378). Data are means $\pm$ SE (n=4). We measured the photosynthesis rate of CMV-L-infected and [CMV-L+Y-sat]-infected and healthy *N. tabacum* with increasing photosynthetic active radiation levels (Fig. 16b and Table 16). The reduction in photosynthesis rate at higher PAR was significant in [CMV-L+Y-sat]-infected plants (CMV-L:15 dpi:1100 µmol/m2/s:Tukey's test, p= 0.026) but not at mid PAR levels (CMV-L:15 dpi:120 µmol/m2/s:Tukey's test, p=0.824).

Stomata conductance in the CMV-O-infected, [CMV-O+Y-sat]-infected, CMV-L-infected, [CMV-L+Y-sat]-infected and healthy plants

Table 17 Stomatal conductance of *N. tabacum* healthy, CMV-O-infected and [CMV-O+Y-sat]-infected plants

PAR value	Healthy			CMV-O			CMV-O+Y-sat		
0	52.5	50.3	80.3	48.4	51.6	58.7	117.3	79.3	63.5
35	120.3	109.5	69.9	53.3	61.9	75.9	157.2	121.2	116.3
50	120.3	105.6	101.5	138.1	148.7	120.3	170	130.5	140.6
60	154.5	131	105.9	109.4	125.9	194.3	153.1	151.9	164.8
75	145.7	144.1	162.4	142.1	137.8	124.8	180.6	113.6	175.3
110	149.4	154.2	149.6	164.4	124.1	123.9	140.5	192.6	180.2
190	200.5	134.4	166.4	128.6	157.5	158.7	175.6	149.2	181.2
1050	290.9	224.2	212.8	208.1	253	209.4	233.2	245.9	289

Unit- mmol H_2O/m2/s

Table 18 Stomatal conductance of *N. tabacum* healthy, CMV-L-infected and [CMV-L+Y-sat]-infected plants

PAR value	Healthy			CMV-L			CMV-L+Y-sat		
0	63.5	99.9	127.2	85.7	122.1	118.9	176.2	95.9	56.5
30	234.1	122.1	181.3	159.2	155.4	227.4	169.3	272.8	156.3
50	174.1	215.6	222.8	130.1	185.4	227.4	231.8	269.3	264.9
75	281.1	176.3	236.5	176.2	239.5	162.6	281.8	250.7	263.6
120	215.5	179	283	205.4	226.5	278.2	253.4	310.2	287.8
1100	330.6	391.6	356.8	444.7	361.6	372.4	320.3	458.8	466.5

Unit- mmol H_2O/m2/s

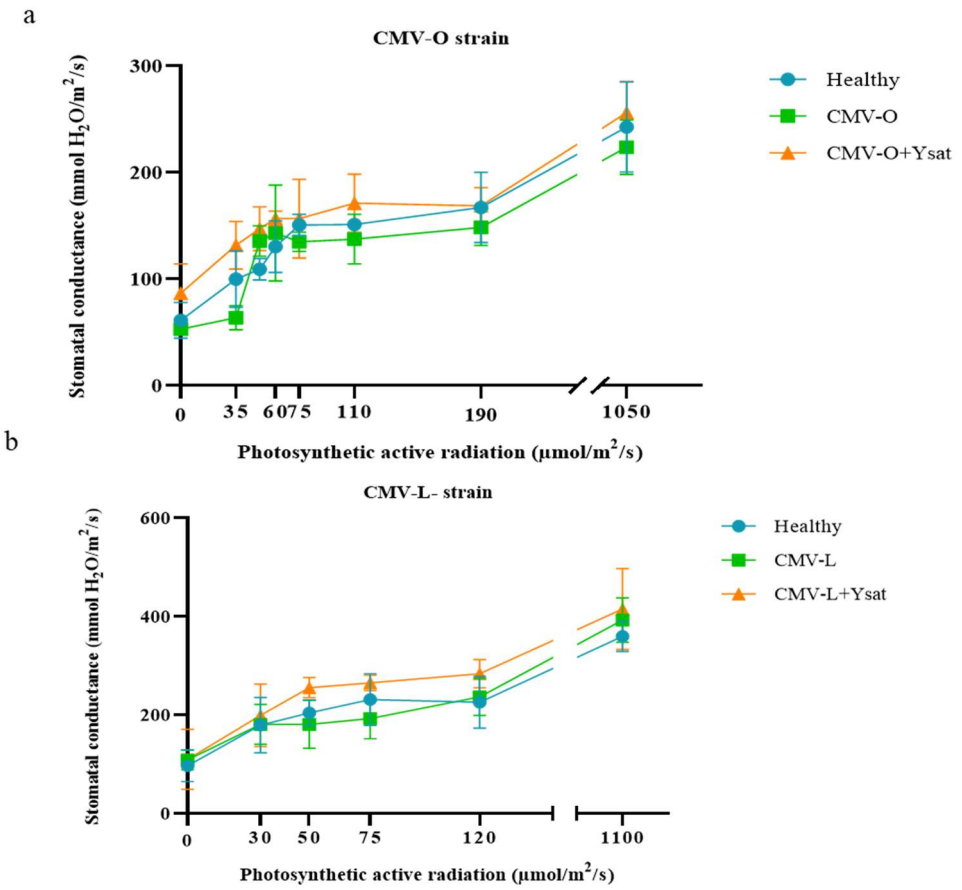

Figure 17 Stomatal conductance at 30 dpi in CMV-infected and [CMV+Y-sat]-infected and healthy plants. Two strains of CMV were used: CMV-O and CMV-L. **a)** Stomatal conductance of CMV-O-, [CMV-O+Y-sat]-infected and healthy *N. tabacum* plants with increasing photosynthetic active radiation levels. Data are means ± SE (n=4). **b)** Stomatal conductance of CMV-L, [CMV-L+Y-sat]-infected and healthy *N. tabacum* plants with increasing photosynthetic active radiation levels. Data are means ± SE (n=3).

We measured the stomatal conductance at 30 dpi CMV-infected and [CMV+Y-sat]-infected and healthy plants. Two strains of CMV were used; CMV-O and CMV-L. We measured the stomatal conductance in the CMV-O-infected, [CMV-O+Y-sat]-infected and healthy *N. tabacum* plants with increasing photosynthetic active radiation levels (Fig. 17a and Table 17). We measured the stomatal conductance in the CMV-L-infected and [CMV-L+Y-sat]-infected and healthy *N. tabacum* plants with increasing photosynthetic active radiation levels (Fig. 17b and Table 18).

Intrinsic rate of increase of aphids grown on CMV-O-infected and [CMV-O+Y-sat]-infected and healthy plants

Table 19 Intrinsic rate of increase of aphid population growth in healthy, CMV-infected and [CMV+Y-sat]-infected *N. tabacum* plants

	Healthy			CMV-O			CMV-O+Y-sat		
	N	d	r_m	N	D	r_m	N	d	r_m
1	4	10	0.102309	4	10	0.102309	4	14	0.073078
2	5	12	0.09898	5	11	0.107979	5	12	0.09898
3	3	10	0.081078	5	11	0.107979	3	10	0.081078
4	4	11	0.093008	4	12	0.085257	5	14	0.08484
5	3	12	0.067565	3	11	0.073707	3	12	0.067565
6	5	12	0.09898	4	10	0.102309	4	13	0.078699
7				6	10	0.132232	4	12	0.085257
8				5	12	0.09898			

r_m=((0.738*log e N)/d) N= number of progeny d= time taken to develop progeny

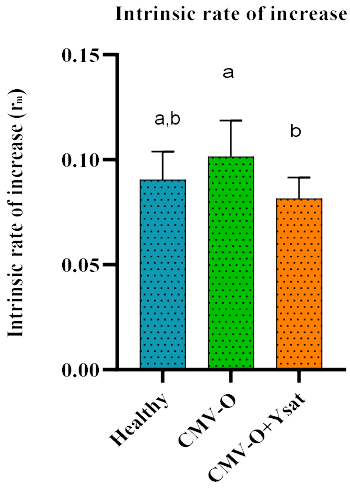

Figure 18 Intrinsic rate of increase (r_m) of *M. persicare* reared on CMV-O-infected, [CMV-O+Y-sat]-infected and healthy plants (the values were 0.101, 0.081 and 0.090, respectively). Different letters are assigned to significantly different results (Tukey's Method at 95% confidence, p=0.0426).

The mean intrinsic rate of increase (r_m) of *M. persicare* reared on CMV-O-infected, [CMV-O+Y-sat]-infected and healthy plants were 0.101, 0.081 and 0.090, respectively. The r_m of *M. persicare* feeding on [CMV-O+Y-sat]- infected plants was significantly low compared to that in the CMV-O- infected plants but did not show any significant difference compared to the healthy plants (Tukey's Method at 95% confidence, p=0.0426) (Fig. 18 and Table 19).

Jasmonic acid levels in CMV-O-infected and [CMV-O+Y-sat]-infected and healthy plants

Table 20 Level of Jasmonic acid in CMV-O-infected and [CMV-O+Y-sat]-infected and healthy *N. tabacum* plants (JA levels in pmol/g)

	Healthy	CMV	CMV+Y-sat
R1	214.691	161.422	130.121
R2	202.673	232.08	237.299
R3	131.46	172.917	209.053
Mean	182.9413	188.8063	192.15767

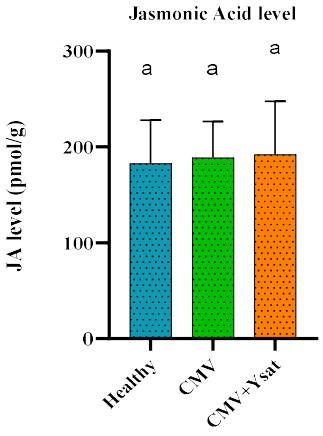

Figure 19 Jasmonic acid levels in healthy, CMV-O-infected and [CMV-O+Y-sat]-infected *N. tabacum* plants. The same letters are assigned to statistically non-significant values (Tukey's Method at 95% confidence, p= 0.9707).

The JA levels in the upper leaves at 1.5 month post inoculation showed no significant difference. The mean JA levels in the healthy, CMV-O-infected and [CMV-O+Y-sat]-infected *N. tabacum* plants were 182.9 pmol/g, 188.8 pmol/g and 192.1 pmol/g, respectively (Tukey's Method at 95% confidence, p= 0.9707).

Level of glucose and sucrose in the CMV-O-infected, [CMV-O+Y-sat]-infected, CMV-L- and [CMV-L+Y-sat]- infected and healthy plants

Table 21 Level of glucose in plant tissues of CMV-O-infected, [CMV-O+Y-sat]-infected, CMV-L-infected and [CMV-L+Y-sat]-infected and healthy plants

Healthy	CMV-O	CMV-O+Y-sat	Healthy	CMV-L	CMV-L+Y-sat
4569.581	1753.276	1900.032	6295.772	2032.12	7251.408
6922.648	5205.566	4059.897	4558.157	4145.524	2565.299
4251.429	1526.617	2557.44	3869.156	4750.079	5947.784
6723.735	10918.36	7938.462			
2322.213	10791.33	3247.883			

Unit- mg/g FW (FW-Fresh wight of the sample)

Table 22 Level of sucrose in the CMV-O-infected, [CMV-O+Y-sat]-infected, CMV-L-infected and [CMV-L+Y-sat]- infected and healthy plants

Healthy	CMV-O	CMV-O+Y-sat	Healthy	CMV-L	CMV-L+Y-sat
4515.66	1419.14	3873.397	2914.404	4666.355	2322.552
5428.32	8768.43	6943.834	5622.869	8370.476	4062.549
1674.39	775.44	1083.69	4070.349	2461.905	5574.124
4639.08	5016.84	2770.02			
1972.44	5058.48	2277.21			

Unit- mg/g FW (FW-Fresh wight of the sample)

a

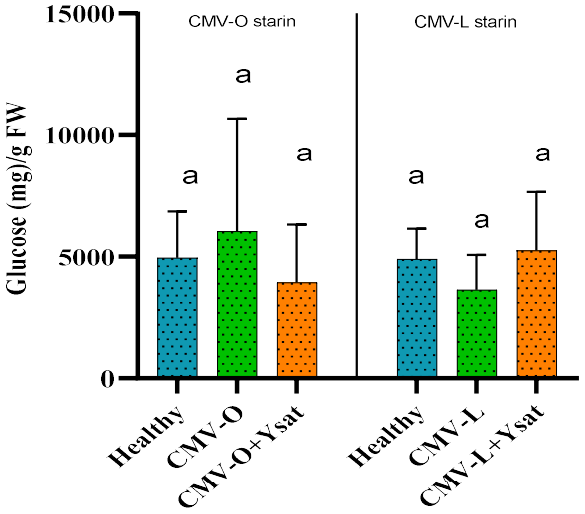

b

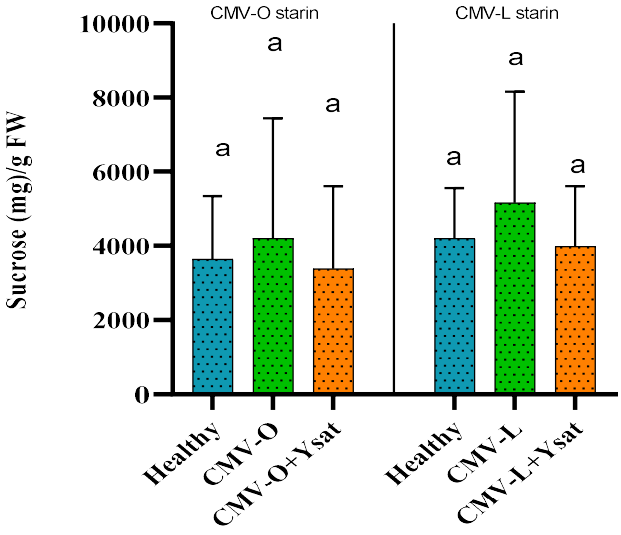

Figure 20 Sugar levels in the CMV-infected and [CMV+Y-sat]-infected and healthy plants. **a)** d-Glucose content did not show any significant difference in CMV-O-infected leaves compare to Y-sat-infected and healthy leaves (n=5, Tukey Method at 95% confidence, p= 0.598). Similar results were obtained when CMV-L strain was used. (n=3, Tukey Method at 95% confidence, p=0.539). **b)** Sucrose content in the leaves of CMV-O-infected, [CMV-O+Y-sat]-infected and healthy plants did not show any significant difference. (n=5, Tukey Method at 95% confidence, p=0.868). Similar results were observed when CMV-L strain was used. (n=3, Tukey Method at 95% confidence, p= 0.776). The same letters are assigned to statistically non-significant values.

The d-Glucose content did not show any significant difference in CMV-O-infected leaves (mean; 6.039 mg/g FW) compare to the Y-sat-infected (mean; 3.94 mg/g FW) and healthy leaves (mean; 4.957 mg/g FW). (n=5, Tukey Method at 95% confidence, p= 0.598). Similar results were observed when CMV-L strain was used. The mean d-Glucose levels in CMV-L-infected leaves, [CMV-L+Y-sat]-infected and healthy leaves were 3.643 mg/g FW, 5.255 mg/g FW and 4.908 mg/g FW, respectively (n=3, Tukey Method at 95% confidence, p=0.539) (Fig. 20a and table 21). The sucrose content in the leaves of CMV-O-infected (mean; 4.207 mg/g FW), [CMV-O+Y-sat]-infected (mean; 3.389 mg/g FW) and healthy (mean; 3.645 mg/g FW) plants did not show any significant difference. (n=5, Tukey Method at 95% confidence, p=0.868). Similar results were observed when CMV-L strain was used. The mean sucrose levels in CMV-L-infected leaves, [CMV-L+Y-sat]-infected and healthy leaves were 5.166 mg/g FW, 3.986 mg/g FW and 4.203 mg/g FW, respectively (n=3, Tukey Method at 95% confidence, p= 0.776) (Fig. 20b and table 22).

Number of alate and apterous aphids on healthy, CMV-O-infected and [CMV-O+Y-sat]-infected *N. tabacum* plants.

Table 23 Number of alate and apterous aphids on healthy, CMV-O-infected and [CMV-O+Y-sat]-infected *N. tabacum* plants.

Healthy		CMV-O		CMV-O+Y-sat	
Alate	Apterous	Alate	Apterous	Alate	Apterous
213	1103	26	724	341	1180

As shown in table 23, the percentage of alate morph and apterous morph on the healthy, CMV-O-infected and [CMV-O+Y-sat]-infected *N. tabacum* plants were 16.19%, 3.47% and 22.42% & 83.81%, 96.53% and 77.58%, respectively. The alate population was significantly higher in Y-sat-infected plants (Chi-square test, p= <0.0001).

Number of alate and apterous aphids on Y-sat-transgenic plant expressing Y-sat dsRNA and wild-type *N. benthamiana* plant.

Table 24 Alate and apterous aphid population on dsY-sat transgenic and wild *N. benthamiana*

Plant type	Y-sat dsRNA transgenic *N. benthamiana*					Wild-type *N. benthamiana*				
Replicate	1	2	3	4	5	1	2	3	4	5
Red aphids	11	9	7	8	10	3	9	4	9	5
Green aphids	23	31	24	20	35	63	49	48	30	39
Total	34	40	31	28	45	66	58	52	39	44

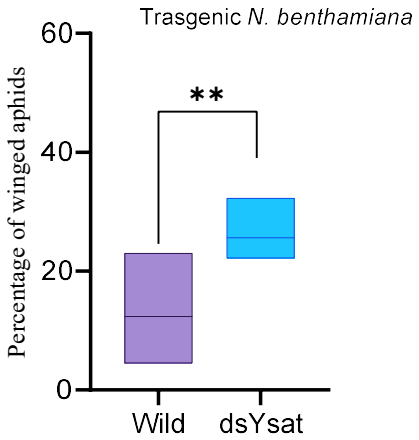

Figure 21 The percentage of alate and apterous morphs of *M. persicare* populations growing on wild-type *N. benthamiana* and Y-sat dsRNA transgenic *N. benthamiana* (dsY-sat).

The percentage of alate and apterous morphs of *M. persicare* populations growing on wild-type *N. benthamiana* and Y-sat inverted repeat expressing transgenic *N. benthamiana* were 11.63% and 26.23% &88.37% and 73.68%, respectively. The alate population was significantly higher on the transgenic plant (Fisher's exact test, p= 0.0007) (Fig. 21).

Number of alate and apterous aphids on *N. benthamiana* leaves where Y-sat dsRNA, plus-sense Y-sat or negative-sense Y-sat were transiently expressed.

Table 25 Fold change data of alate and apterous aphids on *N. benthamiana* leaves which were agroinfiltrated with the GUS, Y-sat (+), Y-sat (-) and Y-sat (dsRNA) Ti plasmid constructs

Treatment	Replicate1	Replicate2	Replicate3	Replicate4
GUS	1	1	1	1
+	0.8	0.77	1.43	1.36
-	1.33	1.29	0.92	0.57
IR	1.84	1.6	1.98	2.01

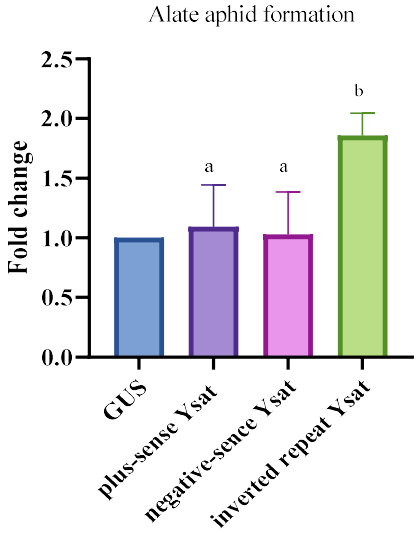

Figure 22 Proportion of alate and apterous morphs of aphid populations feeding on transiently expressed Y-sat dsRNA, plus-sense Y-sat (+) and negative-sense Y-sat (-) *N. benthamiana* leaves. The GUS gene was used as the control.

Experiment was conducted four times, and the data represent the fold change number of alates in each treatment corresponding to the respective control. The same letters are assigned to statistically non-significant values. Only the aphids feeding on the leaves where Y-sat-IR was transiently expressed showed a significantly higher number of alates (n=4, Dunnet's test at 95% confidence, p= 0.0018) (Fig. 22 and Table 25).

Wing induction study on transgenic *N. benthamiana* expressing plus-sense Y-sat, negative-sense Y-sat, and wild-type plant.

Table 26 Number of alate and apterous on the transgenic *N. benthamiana* expressing plus-sense Y-sat, negative-sense Y-sat, and wild-type plants

	Replicat1 (n-30)		Replicat2 (n-30)		Replicat3 (n-30)		Replicat4 (n-25)	
	#red	%	#red	%	#red	%	#red	%
Y-sat (+)	1/23	4.34%	2/19	10.5%	1/21	4.7%	2/19	10.5%
Y-sat (-)	0/18	0%	2/21	9.5%	3/22	13.63%	2/20	10%
Wild	2/21	9.5%	2/23	8.6%	1/21	4.7%	2/19	10.5%

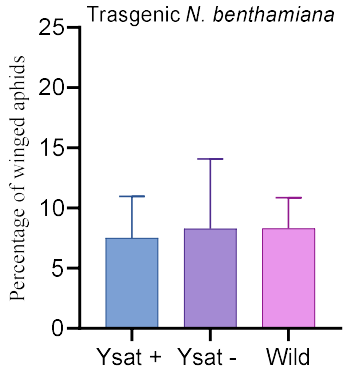

Figure 23 The percentage of alate and apterous morphs of *M. persicare* populations growing on the wild-type *N. benthamiana* and Y-sat plus-sense and minus-sense expressing transgenic *N. benthamiana*

Both transgenic plants did not induce alate development significantly, differently from that of wild-type plant (n=4, Tukey's test at 95% confidence, p= 0.9513) (Fig. 23 and Table 26).

Effect of Y-sat dsRNA on aphid wing formation by artificial feeding.

Table 27 Percentages of alates in the artificial feeding with different dsRNAs

	Percentage of winged aphids		
	Control	Y-sat	LYSV
Experiment 1 (n-30)	35.2%	50%	29.4%
Experiment 2 (n-30)	29.4%	46.6%	37.5%
Experiment 3 (n-30)	37.5%	41.1%	29.4%
Experiment 4 (n-30)	38.8%	43.7%	37.5%
Experiment 5 (n-25)	28.5%	35.7%	30.7%

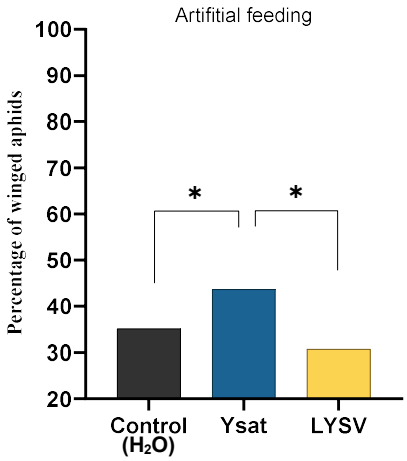

Figure 24 Proportion of alate and apterous morphs of aphid populations feeding on an artificial diet consisting of Y-sat dsRNA and LYSV (control for dsRNA). H_2O was used as a negative control.

Proportion of alate and apterous morphs of aphid populations feeding on an artificial diet consisting Y-sat dsRNA was significantly higher compared to the leek yellow strip virus (LYSV) dsRNA and dH_2O treatments. Statistical significance was determined by two-way ANOVA with Tukey's multiple comparison test. *, $p \leq 0.05$ (Fig. 24 and Table 27).

RT-q-PCR for *Apns1* in aphid

Table 28 Expression levels of *Apns1* mRNA in aphids feeding on the dsY-sat transgenic and wild-type *N. benthamiana* plants

Apterous-3rd-Nymph	Alate-Adult (A(1))	Apterous-Adult (A(1))	Alate-3rd-Nymph	Apterous-3rd-Nymph	Alate-Adult (A(1))	Apterous-Adult (A(1))
1.442924	1	1.064229	2.859814	2.487306	2.43662	1.325817
1.761124	1.048588	1.159553	3.422871	1.887013	1.95519	1.448047
1.878501	1.219227	1.020103	2.582248	2.235445	2.828249	1.493594
2.524043	0.875789	1.092137	2.717914	1.809926	2.11987	1.890367

Values are fold change

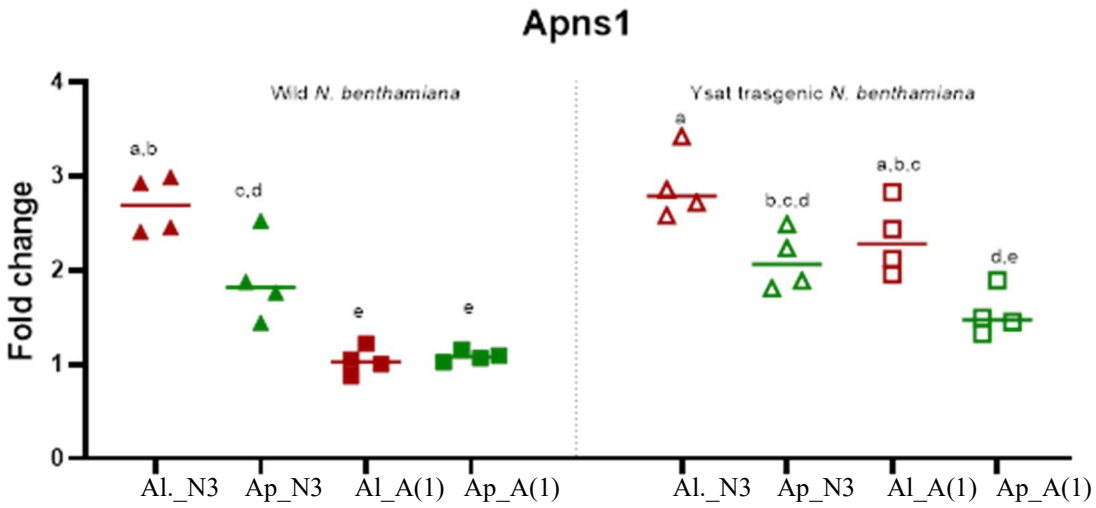

Figure 25 Relative expression of the *Apns1* mRNA in the 3rd instar and early adult stage (A(1)) of alate and apterous morphs feeding on wild-type and dsYsat expressing transgenic *N. benthamiana*. Al-alate morph, Ap-apterous morph

In both treatments, alates at the 3rd instar, the expression of *Apns1* was higher than that of apterous morph. When nymphs develop into the early adult stage (A(1)), the *Apns1* expression reduced significantly and did not show any significant difference among alate and apterous morphs in wild-type *N. benthamiana,* but on the dsY-sat transgenic plants at the A(1) stage of alate morph did not significantly reduce the *Apns1* gene expression and maintained at a higher level compared to that on wild-type plants (n=4, Tukey Method at 95% confidence, p= <0.0001). The same letters are assigned to statistically non-significant values.

RT-q-PCR for Dynein heavy chain 7 in aphids

Table 29 Expression levels of dynein heavy chain 7 mRNA in aphids on healthy, CMV-O-infected, [CMV-O-+Y-sat]-infected *N. tabacum* plants

Healthy	CMV-O	[CMV-O-+Y-sat]-
1.293939	1.215173	0.68283
1.360296	3.542914	0.651395
0.760759	1.159467	0.619041
0.713493	2.353438	1
1.547243	4.311709	1.46484
0.860642	2.459026	1.162892

Values are fold change

Relative expression of the dynein heavy chain 7 mRNA in a single aphid feeding on healthy, CMV-O-infected, [CMV-O-+Y-sat]-infected *N. tabacum* plants. Aphids feeding on CMV-O-infected plants showed a significant elevation in the expression while aphids feeding on Y-sat-infected plants showed a neutral change in expression compared to the healthy treatment (n=6, Tukey Method at 95% confidence, p= 0.0055) (Table 29).

sRNA data analysis.

Table 30 Length distribution of sRNA reads generated in aphids feeding on wild-type and dsY-sat transgenic *N. benthamiana* and CMV-infected and [CMV+Y-sat]-infected *N. tabacum*.

Size (nt)	Wild type	dsY-sat transgenic	CMV	CMV+Y-sat
18	0.132752	0.139648	0.171505	0.188364
19	0.111269	0.114961	0.194286	0.204213
20	0.303734	0.334143	0.576808	0.576529
21	0.845355	0.996572	1.600313	1.57604
22	12.94156	15.91205	19.52952	18.99231
23	22.87366	18.12557	11.41789	11.06545
24	10.70337	11.50962	12.53529	12.48175
25	22.71434	27.29881	25.0689	27.66517
26	5.195086	5.065049	4.993256	4.794326
27	3.871681	3.472948	3.522686	3.219157
28	3.271692	2.749753	2.99101	2.70826
29	4.152369	3.351058	3.625985	3.367023
30	3.755831	3.322535	3.874443	3.63526
31	2.856656	2.305934	2.501532	2.316128
32	2.330657	1.726571	2.142728	1.879429
33	2.257695	2.173958	3.617571	3.680902
34	0.098971	0.080044	0.141543	0.145671
35	1.583311	1.320772	1.494732	1.504017

Values are percentages of sRNA of different sizes aligned to the *M. persicare* genome (AphidBase, BIPAA).

The length distribution of sRNA generated in aphids feeding on wild-type *N. benthamiana*, dsY-sat transgenic *N. benthamiana*, CMV-O-infected *N. tabacum* and [CMV-O+Y-sat]-infected *N. tabacum,* aligned to *M. persicare* genome (AphidBase, BIPAA) are shown in the table 30. The data shows that the 25nt is the peak sRNA size in aphids. These values are used to construct Fig. 26a.

Table 31 Length distribution of sRNA reads generated in aphids feeding on dsY-sat transgenic *N. benthamiana* and [CMV+Y-sat]-infected *N. tabacum*

Size (nt)	Feeding on dsY-sat transgenic *N. benthamiana*	Feeding on [CMV-O+Y-sat]-infected *N. tabacum*
18	0.072307	0.204082
19	0.072307	0.204082
20	0.144613	0.153061
21	0.433839	0.816327
22	1.446132	1.22449
23	0.723066	1.173469
24	3.326103	3.061224
25	8.966016	8.265306
26	11.85828	11.12245
27	11.71367	11.9898
28	12.14751	15.15306
29	12.50904	13.52041
30	10.9906	9.387755
31	7.447578	8.112245
32	8.387563	6.989796
33	8.170644	7.244898
34	0.21692	0.306122
35	1.373825	1.071429

The values are percentage reads aligned to the Y-sat sequence.

When sRNAs in aphids were aligned to the Y-sat sequence (Y-sat-derived sRNA), the peak sizes were around 25-31nt (Table 31). These values are used to construct the Fig. 26b.

Table 32 Length distribution of sRNA reads generated in aphids feeding on CMV-O-infected and [CMV-O+Y-sat]-infected *N. tabacum*

Size (nt)	Feeding on CMV-O-infected *N. tabacum*	Feeding on [CMV-O+Y-sat]-infected *N. tabacum*
18	0	0
19	0.325203	0
20	0.325203	1.020408
21	0.97561	2.040816
22	4.227642	1.020408
23	5.203252	8.163265
24	16.58537	14.28571
25	15.28455	18.36735
26	10.89431	8.163265
27	10.4065	13.26531
28	10.89431	6.122449
29	6.666667	5.102041
30	7.479675	8.163265
31	4.390244	5.102041
32	2.439024	4.081633
33	2.276423	3.061224
34	0	0
35	1.626016	2.040816

The values are percentage reads aligned to the CMV genome.

Data in table 32 shows that the peak size of sRNA which were mapped to CMV genome are 24 and 25nt long. This is shorter than that of the sRNA mapped to Y-sat. These values are used to construct the Fig. 26c.

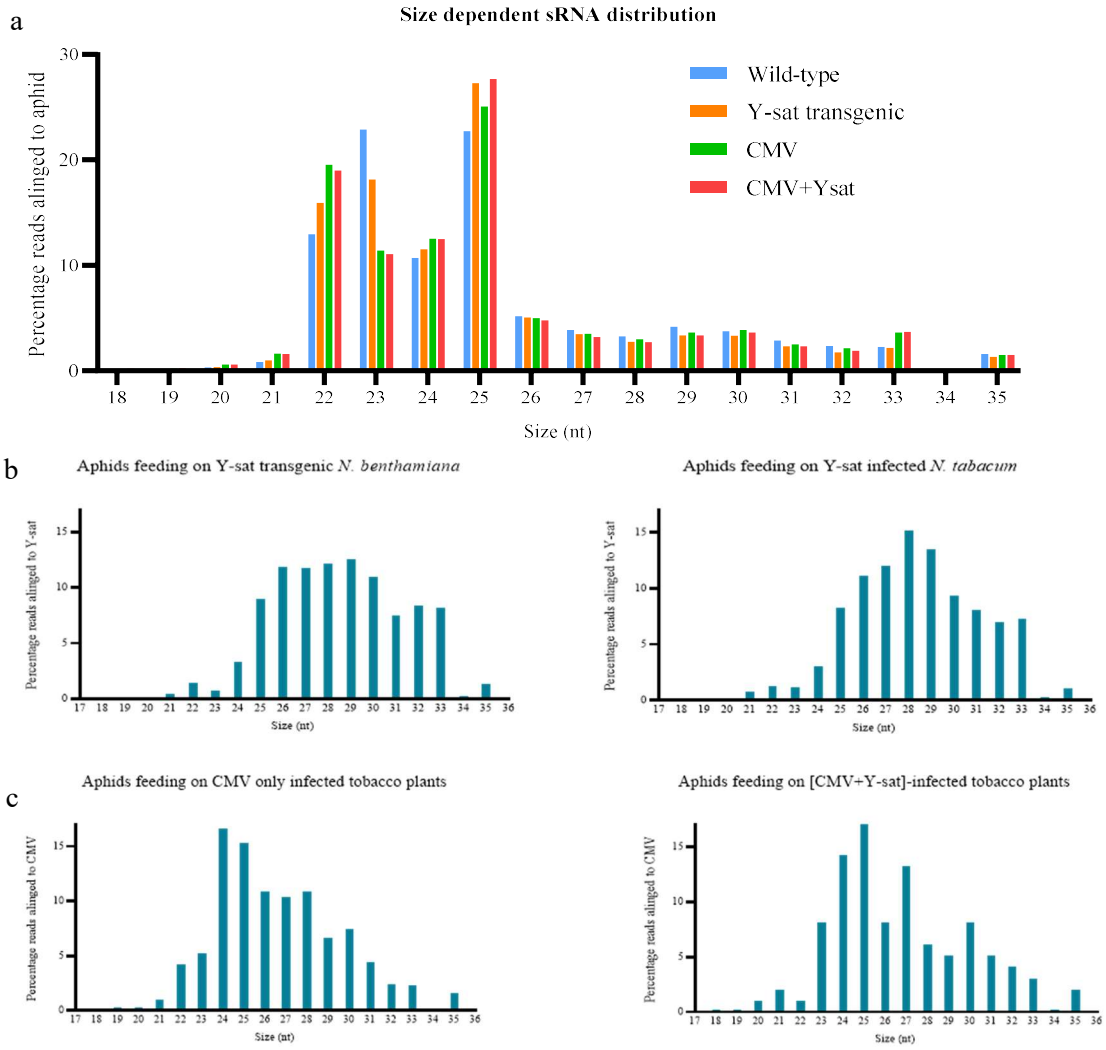

Figure 26 a) Length distribution of small sRNA reads generated in aphids, which aligned to *M. persicae* (AphidBase, BIPAA). Aphids were grown for several generation on wild-type and dsYsat transgenic *N. benthamiana* and CMV-infected and [CMV+Y-sat]-infected *N. tabacum*. Values are the percentage of reads. b) Length distribution of sRNA reads generated in aphids, which aligned to Y-sat. Aphids were grown for several generation on dsYsat transgenic *N. benthamiana* and [CMV+Y-sat]-infected *N. tabacum*. Values are the percentages of the reads of each size aligned to the Y-sat. c) Length distribution of small sRNA reads generated in aphids, which aligned to CMV. Aphids were grown for several generation on CMV-O-infected and [CMV-O+Y-sat]-infected *N. tabacum*. Values are the percentage of reads of each size aligning to the CMV genome.

Length distribution of sRNA in aphids feeding on different treatments showed that the aphid processes dsRNA into different sizes depending on the treatment. The peak size of sRNA processed in aphids feeding on the CMV-infected plants ranged from 23-27nt (Table 32, Fig. 27b). In contrary, the peak size of sRNA processed in aphids feeding on the [CMV+Y-sat]-infected plants or Y-sat transgenic ranged from 26-29nt (Table 31, Fig. 27c). The Y-sat resulted longer sRNA in aphids.

RT-q-PCR for CMV in infected plants

Table 33 Relative CMV-O- levels of CMV-O-infected and [CMV-O+Y-sat]-infected plants determined by quantitative real-time PCR

Replicate	CMV-O	CMV-O+Y-sat
1	0.028487	0.001066
2	0.020551	0.001749
3	0.01406	0.001059
4	0.006622	0.001686
5	0.012384	0.000483
Mean	0.016	0.0012

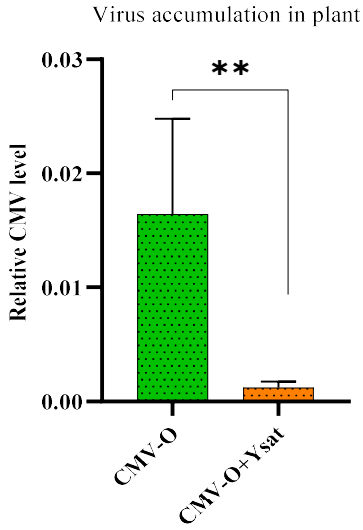

Figure 27 Relative CMV-O levels of CMV-O-infected and [CMV-O+Y-sat]-infected plants determined by quantitative real-time PCR.

The RNA level of 18S was used for the data normalization. CMV-O accumulation was significantly lower in [CMV-O+Y-sat]-infected plants (t-test, P=0.0037). **P<0.05 (Fig. 27 and Table 33).

Transmission of CMV from CMV-O-infected and [CMV-O+Y-sat]-infected plants

Table 34 Virus transmission efficiency from CMV-O-infected and [CMV-O+Y-sat]-infected plants

	R1	R2	Infected %
CMV-O	9/10	8/10	85%
CMV-O + Y-sat	6/10	5/10	55%

Transmission efficiency from CMV-O-infected and [CMV-O+Y-sat]-infected were 85% and 55%, respectively and significantly different (chi-square test, p=0.038). **P<0.05 (Table 34). When plants are infected with Y-sat the transmission is significantly reduced from 85% to 55%.

RT-q-PCR for CMV in individual aphid

Table 35 Relative CMV level in a single aphid feeding on CMV-O-infected and [CMV-O+Y-sat]-infected plants

Individual aphid	CMV-O	CMV-O+Y-sat
1	1	0.407042
2	0.334868	0.369915
3	0.665858	0.209504
4	1.191611	0.533034
5	0.889097	0.332797
6	1.187715	0.265588
7	1.050757	0.497064
8	2.124654	0.254696
9	0.657604	0.081451
10	0.832966	0.543783
11	0.725232	0.573703
Mean	0.969124	0.369871
SE	0.132237	0.04549

CMV levels in a single aphid fed on [CMV+Y-sat]-infected plants were only 2.6 times lower than those in a single aphid fed on CMV-infected plants. (t-test, P=0.0006). ***P<0.01 (Table 35)

RT-q-PCR for *ABCG4* gene in alate aphids

Table 36 Expression of *ABCG4* gene in winged aphids feeding on CMV-O-infected and [CMV-O+Y-sat]-infected *N. tabacum* plants

Y-sat_N3	CMV_N3	Y-sat_A(1)	CMV_A(1)	Y-sat_A(4) (Winged)	CMV_A(4) (Winged)
1.0000	0.523226	0.994933	0.758599	9.723406	10.59851
1.008392	0.691007	1.514837	0.956822	10.24957	10.0228
1.316336	0.77508	1.681807	0.947787	8.415168	8.19018
1.19198	0.923029	1.353811	0.778898	9.05985	8.220367

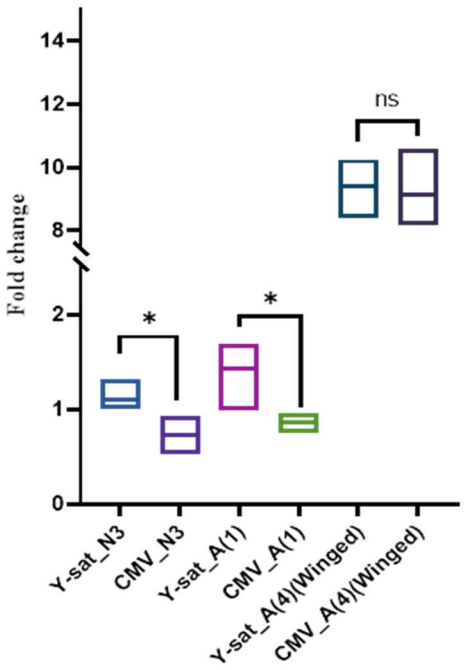

Figure 28 Expression of the *ABCG4* gene in aphids. Two-sided t test showed that the expression of *ABCG4* gene is significantly increased in the nymphal instars of aphids feeding on the Y-sat-infected plants. (N3 [p=0.0122], A(1) [p=0.15] and A(4) [p=0.8923]).

In general, the gene *ABCG4* expression is higher at late adult stage (A(4)) while at early adult stage (A(1)) and N3, the expression is lower. In the nymphal instar, the expression of *ABCG4* gene in aphids feeding on CMV-O-infected and [CMV-O+Y-sat]-infected plants showed a significant difference. In both N3 and A(1) stages the aphids growing on Y-sat-infected plants showed a significantly higher expression of *ABCG4* than that of the aphids growing on CMV-infected plants. The expression level at A(4) did not show any significant deference (Table 36, Fig. 28).

Observation of aphid colour change

A unique descent of body colour and wing formation in *M. persicare* have been revealed in this study (Fig. 11). The colour variation in the body can be observed in the three to four day-old aphids (Fig. 29). Apterous and alate adult females are shown in Fig. 30. During this study, sexual reproduction of *M. persicare* was not observed and did not find any eggs. Therefore, based on the data, the viviparous life cycle of the *M. persicare* is presented (Fig. 31).

Figure 29 Body colour variation at 3day-old aphids.
Red (top) and green (bottom) morphs

Figure 30 Adult alate [A(4)] and apterous [A(2)] females of *M. persicare*

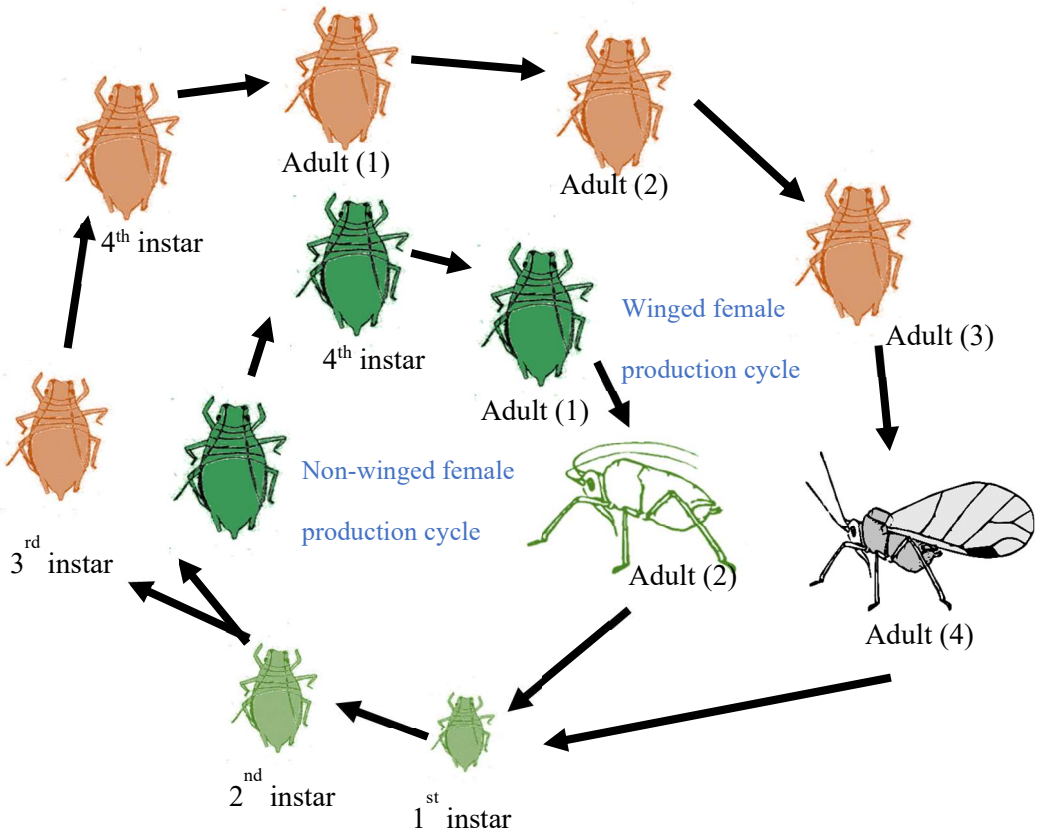

Figure 31 The viviparous life cycle of *M. persicare*

RT-q-PCR for *ABCG4* gene in aphids feeding on dsY-sat transgenic plants

Table 37 Expression levels of *ABCG4* mRNA in aphids feeding on the dsY-sat transgenic and wild-type N. benthamiana plants

Wild-type				dsY-sat transgenic			
Alate-N3	Apterous-N3	Alate-A(1)	Apterous-A(1)	Alate-N3	Apterous-N3	Alate-A(1)	Apterous-A(1)
0.831969	0.818142	0.914726	0.608888	1.217963	1	1.624589	0.897602
0.760886	0.515349	0.78275	0.661205	1.429875	0.708251	1.453244	1.180429
0.99962	0.333867	1.154865	0.447888	1.194185	0.80822	1.320186	0.783495
0.704128	0.466755	0.877728	0.531509	1.343107	0.693646	1.06302	0.618305

Values are fold change

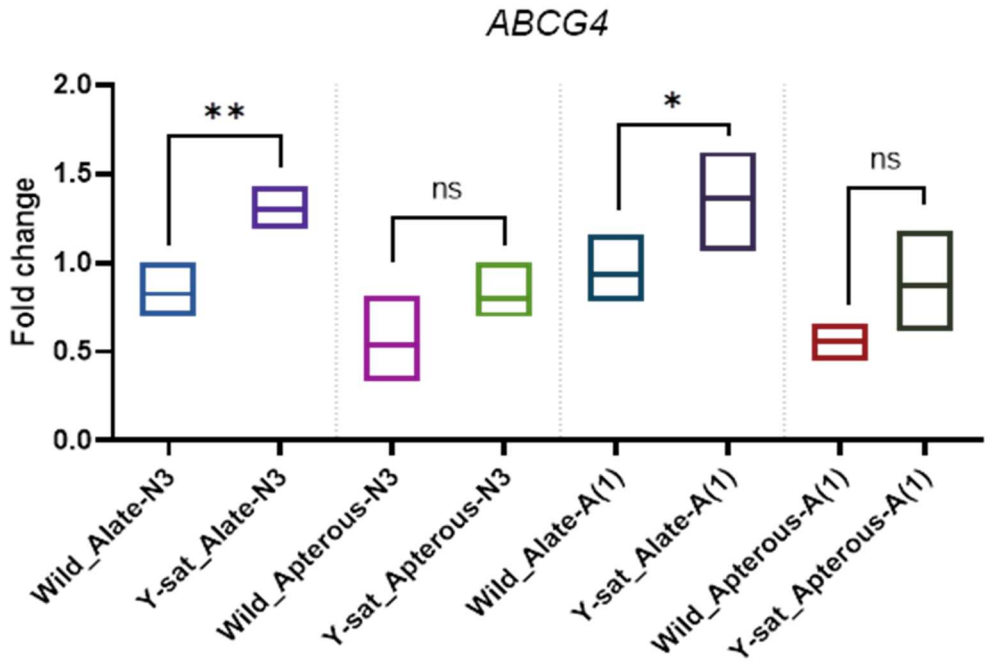

Figure 32 The relative expression of the *ABCG4* gene in aphids feeding on wild-type and dsY-sat transgenic *N. benthamiana*.

The *ABCG4* mRNA in N3 and A(1) (4-5 days after N3) of alate and apterous morphs feeding on wild type and Y-sat IR transgenic *N. benthamiana* is shown in table 37 and figure 32 *ABCG4* is significantly highly expressed in alate aphids feeding on dsY-sat transgenic plants at both development stages 3rd instar (N3) and early adult (A(1)) stages (N3- p=0.0014; A(1)- p= 0.0029). There was no significant difference in apterous aphids.

RNA dot blot hybridization for *in-vitro* binding of miR9b into Y-sat and *ABCG4*

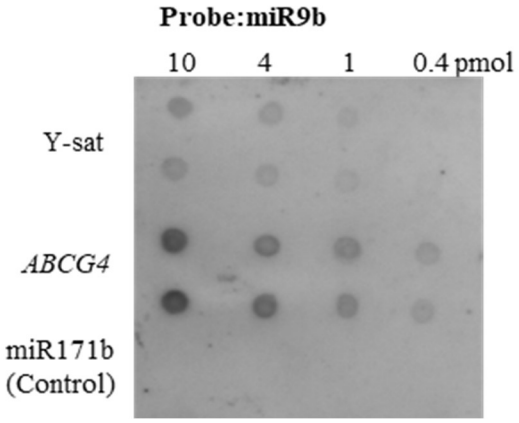

Figure 33 Dot blot hybridization showed that both Y-sat and *ABCG4* are interacting with miR9b. The first spot is equivalent to 10 pmol of RNA, others are 10-fold dilutions. miR171b was used as a negative control.

RNA dot blot assay was performed to find the ability of miR9b, the micro-RNA responsible for regulation of *ABCG4* gene. Both synthetic sRNA of Y-sat and ABCG4 of a serial dilution (10, 4, 1, 0.4pmol) were probed with miR9b. miR17b was used as negative control. The dot blot hybridization showed that the miR9b could interact with both the Y-sat and *ABCG4* (Fig. 33).

DISCUSSION

Y-sat depends on cucumber mosaic virus (CMV) for its replication and encapsidation (Shimura et al. 2011). The presence of Y-sat in CMV-infected tobacco plants change normal mosaic symptoms into bright yellowing of leaves (Figure 8). This is done by down-regulating the *ChlI* mRNA, which results in reduction in chlorophyll biosynthesis in tobacco plants (Shimura et al. 2011), consequently causing bright yellowing of leaves. It has been shown that the Y-sat is unable to compete with other similar size satRNAs (Masuta et al. 1990).

Both CMV and Y-sat are transmitted by aphid species such as *Aphis gossipii* and *M. persicae* (green peach aphid) (Escriu et al. 2000; Ziebell et al. 2011). CMV is non-persistently transmitted by binding loosely to the receptors in the acrostyle of the aphid (Webster et al. 2018). Although, recent works have improved the knowledge of the coevolution of viruses, hosts and vectors, we still do not know it is unknown how satRNAs have shaped the coevolution of the virus, host and vector (Wang et al. 2017; Carr et al. 2018).

Aphid attraction towards plants showing Y-sat-mediated yellow symptoms

We tested whether *M. persicare* is differently attracted to tobacco plants which showed bright yellow symptoms by using a pairwise bioassay between CMV-O-infected and [CMV-O+Y-sat]-infected plants. The results indicate that tobacco plants infected with [CMV+Y-sat] attracted significantly more aphid vectors to tobacco compared to the CMV-only-infected or healthy plants (Fig 13). Bright yellow leaves will easily attract aphids (Kennedy et al. 1961b; Macias and Mink 1969) to tobacco plants so that the aphids will invest less cost in host selection.

An olfactory bioassay was conducted to find the effect of volatile organic compounds (VOCs) on the aphid attraction. Different pairs of treatments were tested in separate experiments. Only around 40% of the tested aphids in each experiment showed attractiveness on either of the plants (Fig. 14). The remaining aphids did not show any preference. We thus confirmed neither CMV infection nor Y-sat infection in tobacco can induce order dependent attraction to aphids.

CMV infection in tobacco can alter the VOCs but not the aphid attraction to the plant (Tungadi et al. 2017). We thus confirmed that the tobacco plants infected with [CMV+Y-sat]-attract a significantly higher number of aphids due to the yellow colour resulted from the Y-sat.

Change in photosynthesis by Y-sat-mediated yellow symptoms

Upon infection of a severe CMV strain, tobacco plants show irregular leaves with deeply indented margins and leaf distortion. This crinkled leaf formation can adversely affect the plant growth and survival. Heavy infection of virus can lead to disruption of chloroplasts in the leaf (Song et al. 2009); however the chloroplast in CMV-infected and Y-sat-infected tissues appeared ultra-structurally indistinguishable, suggesting that the chloroplast is not severely damaged (Masuta et al. 1993).

Effect of CMV-infection and [CMV+Y-sat]-infection on photosynthesis in tobacco was tested by measuring photosynthetic rate under several different light intensities at 15 dpi and 30 dpi. The experiment was carried out using two CMV strains (CMV-O and CMV-L). At 30 dpi there was no significant difference (Table 14 and Fig. 15). It was evident that at early stage of growth (15 dpi), there is a significant reduction in photosynthesis in Y-sat-infected plants but not always (Table 15 and Fig. 16). The results indicate that yellow pigments somehow compensate for the photosynthesis rate, giving only a little disadvantage to the plant.

In order to maintain the photosynthesis rate at a normal rate in Y-sat-infected plants, the stomatal conductance of the plants infected with CMV and [CMV+Y-sat] is maintained at a higher level (Table 17,18 and Fig. 17).

Effects of Y-sat on aphid growth and survival

An intrinsic rate of increase (r_m) provides how aphid population growth differs under different treatments and the r_m of aphid population on [CMV-O+Y-sat]-infected tobacco plants were significantly different from that of CMV-O-infected plants but similar to the healthy plants.

Therefore, the aphid population growth on Y-sat-infected plants has no difference compared to the that of the healthy plants (Table 19 and Fig. 18).

Jasmonic acid (JA) functions as a central signal in plant defence against herbivore insects including production of nicotine (Diaz-Pendon et al. 2007; Ziebell et al. 2011). The level of JA in all treatments did not show any significant difference (Table 20 and Fig. 19). This indicates that there is no effect of Y-sat on the plant JA-mediated resistance to aphid.

Phloem sap also plays a major role in aphids' likelihood to continue feeding on the plant. An increase in sugar content of phloem sap enhances the aphids' growth on plants (Jakobs and Müller 2018). The levels of sucrose and d-glucose in infected and healthy plant leaves were measured using two CMV strains (CMV-O and CMV-L). Neither the levels of d-glucose nor sucrose in the healthy, CMV-infected and [CMV+Y-sat]-infected *N. tabacum* plants for both CMV strains showed any significant difference (Table 21 and 22 and Fig. 19 and 20).

Change in alate and apterous morph production of *M. persicare* by Y-sat

Furthermore, the number of the alate and apterous morphs in *M. persicare* populations growing CMV-O-infection, [CMV-O+Y-sat]-infected and healthy *N. tabacum* plants were significantly different. This was initially observed by the comparison of red and green morphs, which developed in colonies growing on the infected and healthy plants. Y-sat infection resulted in a significantly higher number of alates (Chi-square test, p= <0.0001). CMV-O-infected *N. tabacum* plants established a safe haven allowing aphids to increase population (Table 23), yet reducing the onward transmission of the virus (Westwood et al. 2013). In order to find out whether the increase in alate morph population is due to Y-sat, the number of alate and apterous morphs of *M. persicare* populations growing on wild *N. benthamiana* and dsY-sat expressing transgenic *N. benthamiana* were measured. We found that the proportion of the alate morph population was more than two-fold in dsY-sat transgenic *N. benthamiana* (Fisher's exact test, p= 0.0007) (Table 24 and Fig. 21) suggesting that the Y-sat somehow affected the wing formation of *M. persicare*.

To further determine the role of Y-sat in aphid wing production, the alate and apterous morphs of *M. persicare* populations feeding on the plants with transiently expressed IR, plus-sense and negative-sense constructs of Y-sat were measured (Table 25). The relative proportion of the alate population in each treatment showed that only dsY-sat could induce alates (Dunnet's test, p= 0.0018) (Fig. 22) suggesting that only dsRNA of Y-sat can induce wing formation in aphids. We observed that the negative and plus-sense Y-sat cannot induce alates. When compared to the aphids feeding on wild-type *N. benthamiana,* the both transgenic plant types did not induce alates significantly (Tukey's test p=0.9) (Table 26 and Fig. 23).

Aphids fed with Y-sat dsRNA in an artificial feeding experiment showed a significantly higher number of alate morph production. Both the control (dH_2O) and dsRNA of leek yellow strip virus (LYSV) did not result any significant increase in alate morph production (Table 27 and Fig. 24), indicating that dsRNA of Y-sat explicitly affected the alate production of *M. persicae* (two-way ANOVA with Tukey's test).

Gene expressions related to wing formation is modified by Y-sat

Our data revealed that the *Apns1* gene in aphids feeding on wild-type *N. benthamiana* and Y-sat transgenic *N. benthamiana* was differentially expressed as follow. In the aphids feeding on wild-type plants, the expression of *Apns1* in the alate 3rd instar (N3) was significantly higher than that of the apterous morph. At the early adult stage (A(1)), the *Apns1* expression was reduced and did not show any significant difference between the alate and apterous morphs. However, in the aphids feeding on the transgenic plants expressing Y-sat dsRNA, the level of the *Apns1* at both the N3 the A(1) stages of the alates were significantly higher than that of the apterous morph. Consequently, *Apns1* in aphids feeding on the Y-sat transgenic plants were maintained at a higher level compared to that of wild plants (Tukey's test p= <0.0001) (Table 28 and Fig. 25). This indicates that Y-sat by some means can maintain the expression of *Apns1* and thereby induce a significantly higher number of alate morph in aphid population.

A homology search of Y-sat nucleotide sequence showed a 25bp-long highly similar sequence to *M. persicare* dynein heavy chain 7 (*dhc7*) mRNA. Dynein heavy chain is a molecular binding protein for movement along microtubules and hence responsible for many general functions (Lupetti et al. 1998; Galigniana et al. 2004; Yang et al. 2008). The expression of *dhc7* mRNA in aphids feeding on the CMV-O-infected, [CMV-O+Y-sat]-infected and healthy *N. tabacum* plants were measured (Table 29). We found that *dhc7* was significantly highly expressed in the aphids feeding on the CMV-O-infected plants (Tukey's test p= 0.0055). Over-expression of *dhc7* might have significant negative effect on aphid. The Y-sat infection has specifically reduced the expression of *dhc7* to a similar level that of the healthy treatment suggesting some negative consequences of overexpression of *dhc7*.

One of the key gene for wing production in aphids has been identified recently (Shang et al. 2020). This gene *ABCG4* was found to be significantly highly expressed in the N3 and A(1) stages of alate aphids feeding on [CMV-O+Y-sat]-infect plants compared to the CMV-O-infected plants (Table 36 and Fig. 28). Similarly, in the N3 and A(1) stages of alate aphids feeding on the Y-sat transgenic plants the *ABCG4* expression was significantly higher (Table 37 and Fig. 32).

sRNA size difference is the likely factor for changes in gene expression

To explore the mechanistic basis of the wing formation, a sequencing analysis of the transcriptomes from the alate and apterous morphs feeding on [CMV-O+Y-sat]-infect *N. tabacum* and Y-sat-transgenic *N. benthamiana* was conducted.

To test whether Y-sat had an impact on the size distribution of *M. persicae*-derived sRNA, the sRNA data was aligned to the *M. persicae* genome. When compared the aphids feeding on all four treatments regardless of the host plant, the Y-sat expression showed a significant increase in long sRNA (Fig. 26a). This showed that irrespective of the host plant, aphids produced much larger sRNA compared to the most common sizes of sRNA generated by dcr-2 in insects (Aliyari et al. 2008; Sabin et al. 2013).

sRNA of aphids fed on [CMV-O+Y-sat]-infected *N. tabacum* and Y-sat-transgenic *N. benthamiana* were mapped to the Y-sat genome to find the size distribution. In both transgenic and infected plants, similar distribution was observed; the 28 and 29nt were the most abundant sizes (Fig. 26b) and when sRNA was mapped to the CMV genome, 24 and 25nt sRNA were the most abundant sizes (Fig. 26c). The difference in size peak shows that the sRNA generated in aphids' body as a response to Y-sat is larger in size than that of generated to CMV. Therefore, it was believed that the 26-31nt long sRNA might mediate the wing formation in aphids and thus explains a higher number of alates in dsY-sat transgenic and Y-sat-infected plants.

Y-sat-mediated wing formation in aphids

As discussed above, three genes which may be important in aphid wing production were studied in detail in this research. We presumed that out of the genes studied, *ABCG4* gene play a key role in Y-sat-mediated aphid wing formation. Our proposing mechanism for Y-sat-mediated aphid wing formation is as fallows.

sRNA-seq data revealed that the aphid produced relatively long siRNAs (Fig. 26) and the siRNAs can be classified as virus-derived PIWI-interacting RNAs (vd-piRNAs). vd-piRNAs are firstly described in drosophila cells and adult mosquitoes as a defensive mechanism (Wu et al. 2010). Insects need to replicate viral RNA genomes into siRNAs of discrete sizes for virus clearance through RNA interference, and vd-piRNAs facilitate this process. Therefore, the long sRNAs present in the aphids feeding on Y-sat-infected plants may be vd-piRNAs only at this point they are satellite-derived piRNAs. It is suggested that these vd-piRNAs are produced through a non-canonical pathway and act redundantly to an antiviral immune response directed by siRNAs (Morazzani et al. 2012; Schnettler et al. 2013).

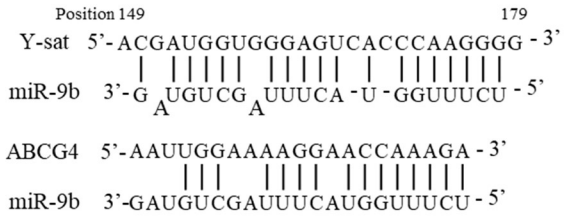

Figure 34 Complementary between aci-miR-9b and Y-sat or *ABCG4*

The vd-piRNAs detected in aphids feeding on the Y-sat-infected plants exhibited a highly complementary sequence to miR9b; the micro-RNA responsible for regulating *ABCG4* (Fig. 34). A higher expression of miR9b down-regulates the expression of *ABCG4* (Shang et al. 2020). We tested our hypothesis by performing a RNA dot blot hybridization, which showed that miR9b could bind to both Y-sat and *ABCG4* (Fig.. 33). Therefore, we presumed that the Y-sat-derived sRNA (vd-piRNAs) in aphid may compete with miR9b and thereby reduce the availability of miR9b which will subsequently over-express *ABCG4*. This will result in a significantly higher number of alate aphids on the Y-sat-infected plants.

Unhindered transmission of Y-sat and CMV by *M. persicare*

Nevertheless, it was anticipated that the transmission of CMV positively correlated with the accumulation of CMV particles in the host tissue. It has been observed that Y-sat greatly reduced the accumulation of CMV as a result of RT-q-PCR. Presence of satRNAs reduces the accumulation of the helper virus which negatively affects the transmission of the helper virus (Escriu et al. 2000). The relative CMV level of Y-sat-infected plants was 13.5 times lesser than that of CMV-only-infected tobacco plants (Table 33 and Fig. 27). Because, Y-sat depends on CMV for its vital functions, this makes Y-sat itself disadvantageous. Under the light of this situation, the frequency of Y-sat transmitted to new hosts would have negatively affected, and the satRNA should have been disappeared with time (Escriu et al. 2000).

Surprisingly, the aphid transmission results showed 55% success in CMV transmission to healthy plants via [CMV-O+Y-sat]-infected plants and 85% success via CMV-O-infected plants (chi-square test, p=0.038) (Table 34). Even though the transmission efficiency was significantly reduced, 55% transmission would be ample for its survival in the nature.

Since the CMV accumulation levels in the plants cannot explain the transmission, the CMV levels of a single aphid stylet feeding on CMV-O-infected and [CMV-O-+Y-sat]-infected tobacco plants were analysed using RT-q-PCR. The results showed that the relative CMV levels in a single aphid feeding on [CMV+Y-sat]-infected plant was only 2.6 times lower than that of a single aphid feeding on the CMV infected plant (t-test, P=0.0006) (Table 35), suggesting that the aphid stylet has a threshold for acquisition of CMV. Furthermore, the CMV levels in aphid stylet explains the efficient transmission of [CMV+Y-sat] to healthy plants.

Quadripartite symbiosis among CMV, aphid and Y-sat

The Y-sat turns host plant leaves bright yellow and influence vector aphids to form more alates by a molecular cross-talk. The hallmark idea of generating more alates is to increase the spread of the virus. The yellow colour attracts significantly a higher number of aphids to [CMV+Y-sat]-infected plants, and an increase number of alate morph promotes the onward transmission of both virus and Y-sat, without compromising the reproduction and survival of the aphid (Fig. 9). Therefore, Y-sat fosters aphid survival while ensuring it's and helper virus's transmission. On the other hand, CMV-only-infected plants can enhance aphid survival but not the spread of the virus.

As explained by Hamilton and Brown's autumn signalling hypothesis (Hamilton and Brown 2001), another advantage of bright leaves is that it act as a warning colour for chewing insects. It has been shown that the autumn senescing in *Betula pubescens* resulted less damage from leaf chewers (Hagen et al. 2003). Under the light of this, Y-sat-infected tobacco plants can gain protection from leaf chewing insect damages while having cross protection from CMV and attenuated symptoms with little effect on photosynthesis.

Use of colour to attract or defend is quite common in animal kingdom. Induction of colour changers in the intermediate host in *Acanthoscephalan parasite* (Bakker et al. 1997; Sparkes et al. 2004; Benesh et al. 2009), colour variation in aphid body (Tsuchida et al. 2010) and warning colouration of *Heterorhabditis*-infected larvae (Fenton et al. 2011) are known to influence the relative susceptibility of the host to predators.

In this study we revealed that CMV is engaged in a quadripartite symbiosis with Y-sat which has given a competitive advantage in the natural selection. Overall, this quadripartite symbiosis shaped by the Y-sat changes a much parasitic relationship into a more mutualistic relationship. Many studies have shown that plant viruses can alter vector behaviour to enhance its spread (Ziebell et al. 2011; Dietzgen et al. 2016; Wu et al. 2017). During the process of evolution, Y-sat has somehow acquired the aphids' attractiveness to yellow colour and its ability to produce alate morph for its advantage, and it is truly remarkable evolutionary adaptation done by a very simple non-cording RNA.

GENERAL DISCUSSION

The sessile nature of plants and hard cell wall, are two most important hurdles faced by plant viruses and satRNAs when it comes to onward transmission. Therefore, nearly all plant viruses and their satRNAs depends on insects, nematodes or fungi for movement from one host to another. Insects, most specifically Hemipteran insects play an important role in plant virus transmission. Aphids (Suborder Sternorrhyncha) are found to transmit nearly 40% of the known plant viruses.

In the processes of transmission, plant viruses and satRNAs have to face numerous constrains, and these constraints apply at all stages of the transmission process namely acquisition, retention and inoculation. First, plant viruses or satRNAs should be spatiotemporally available to the vector. Second, after ingestion by the vector, the particles should be retained by the vector until it passes to a new host. Furthermore, the plant viruses and satRNAs have to face the constraints at the scale of the ecosystem. Competition for the vectors, adaptation to the vectors, adaptation to the hosts and the interactions between the host and vector are some of them.

Evolution through symbiotic relationships might be the best suitable strategy to overcome the above constrains. The term symbiosis implies both mutualistic symbiosis or antagonism symbiosis. These relationships can even be obligate. In this thesis, the evolution of symbiotic relationships in a plant virus and a satRNA was explained in detail.

In the chapter one, the OYDV-S isolate has clearly lost the ability to be transmitted via aphids. Yet the isolate is well spread and survived in Hokkaido. It was truly remarkable to observe that a virus isolate which has lost the most essential feature for survival is somehow able to abundantly exist in the nature. The HC-Pro plays an important role in binding the virus particle to the stylet receptors acting as a bridge protein between the two. The mutation in the HC-Pro in the OYDV-S isolate has lost this critical function and therefore OYDV-S particles may not retain in the aphid stylet. It was also observed that OYDV-S always coinfected with LYSV. Therefore, we tested whether the LYSV HC-Pro can bind to OYDV CP. The data of the pull-down analysis using a

His-affinity gel and Far-Western dot blot analysis showed that OYDV-S CP is able to bind to the HC-Pro of LYSV. Therefore, we presumed that LYSV HC-Pro works *in trans* as a platform that interlinks both LYSV and OYDV-S to the aphid stylet.

The symbiotic interaction with OYDV-S and LYSV is a clear adoption evolved by OYDV-S to overcome the inability of attaching the virus particles in the aphid stylet. Further, the mutation in HC-Pro have resulted in a reduced RSS activity leading to less severe symptoms in the garlic plants. Under the man-made selection pressure, the plant viruses of cultivated plants, which produce mild symptoms, are more likely to be survived while plants with severe symptoms are easily detected and removed.

In the chapter two, a symbiotic interaction established by a satRNA is redefined. The studied satRNA is Y-sat, which use CMV as the helper virus. satRNAs are non-cording RNAs which can affect the accumulation and symptomatology of the helper virus. Y-sat specifically down-regulates the *ChlI* mRNA, impairing the chlorophyll biosynthesis in *Nicotiana* plants and thus causing bright yellow symptoms. However, our photosynthesis measurements showed that this yellow colouration has little effect on photosynthesis. The CMV level in Y-sat-infected plants are 13 times lower than CMV-only-infected plants, but our transmission experiments showed that the transmission rate was not strongly affected by the CMV levels.

The dsRNA of Y-sat was found to produce sRNA which can affect the morphology of the aphids. There was a significant higher number of alate aphids on Y-sat-infected plants compared to the CMV-only-infected and healthy plants. The winged aphid production must be very important to spread the Y-sat to other hosts.

We believe that this is a cleaver pull and push strategy deployed by Y-sat. The number of vectors is limited in an ecosystem and the vectors sequentially acquire viruses where the transmission of the latter may reduce (Fereres 2007). The yellow colour will attract more aphids to the Y-sat-infected plants giving a competitive advantage to win the competition with other viruses for the

vectors. Secondly the disperse of the vectors to new host is efficacity achieved by inducing the aphids to produce more alates.

Finally, we believe that we could successfully demonstrate two examples of well-organized symbiotic interactions driven by either a plant virus or a satRNA to indicate how organisms have coevolved symbiotic interactions to ensure their survival.

SUMMERY

Viruses and the satellite RNAs have found to modify plant-virus-vector interactions at all possible levels and these modifications have often strengthened their fitness for their survival. In this thesis, two symbiotic interactions, which coevolved targeting the upsurge of aphid transmissibility, are documented.

The chapter one explains how helper component protease (HC-Pro) of leek yellow stripe virus facilitate the aphid transmission of an onion yellow dwarf virus isolate with a mutated HC-Pro gene. It is presumed that LYSV HC-Pro works *in trans* as a platform that interlinks both LYSV and OYDV with the aphid stylet.

In the chapter two, evolution of a quadripartite symbiosis driven by a satellite RNA to promote aphid transmission was explained. Y-sat develops a quadripartite symbiotic interaction among cucumber mosaic virus, tobacco plant and aphid. Based on the data derived in this study it is clear that Y-sat regulates both the host plant and the insect vector via molecular crosstalk in order to deploy a pull-push strategy against aphids. The pull-push strategy enhances the spread and survival of both CMV and Y-sat.

These are two examples of manipulations made by a plant virus and a satellite RNA via symbiotic interactions to ensure their survival.

REFERENCES

Aliyari R, Wu Q, Li HW, Wang XH, Li F, Green LD, Han CS, Li WX, Ding SW (2008) Mechanism of Induction and Suppression of Antiviral Immunity Directed by Virus-Derived Small RNAs in Drosophila. *Cell Host Microbe* 4:387–397

Arya M, Baranwal VK, Ahlawat YS, Singh L (2006) RT-PCR detection and molecular characterization of Onion yellow dwarf virus associated with garlic and onion. *Curr Sci* 91:1230–1234

Atreya CD, Pirone TP (1993) Mutational analysis of the helper component-proteinase gene of a potyvirus: Effects of amino acid substitutions, deletions, and gene replacement on virulence and aphid transmissibility. *Proc Natl Acad Sci U S A* 90:11919–11923

Bakker TCM, Mazzi D, Zala S (1997) Parasite-Induced Changes in Behavior and Color Make Gammarus Pulex More Prone to Fish Predation. *Ecology* 78:1098

Benesh DP, Seppala O, Valtonen ET (2009) Acanthocephalan size and sex affect the modification of intermediate host colouration. *Parasitology* 136:847–854

Blanc S, Ammar ED, Garcia-Lampasona S, Dolja V V., Llave C, Baker J, Pirone TP (1998) Mutations in the potyvirus helper component protein: Effects on interactions with virions and aphid stylets. *J Gen Virol* 79:3119–3122

Carr JP, Murphy AM, Tungadi T, Yoon JY (2018) Plant defense signals: Players and pawns in plant-virus-vector interactions. *Plant Sci.* 279:87-95

Diaz-Pendon JA, Li F, Li W-X, Ding S-W (2007) Suppression of antiviral silencing by cucumber mosaic virus 2b protein in Arabidopsis is associated with drastically reduced accumulation of three classes of viral small interfering RNAs. *Plant Cell* 19:2053–63

Dietzgen RG, Mann KS, Johnson KN (2016) Plant virus-insect vector interactions: Current and

potential future research directions. *Viruses* 8:303

Dolja V V, Herndon KL, Pirone TP, Carrington JC (1993) Spontaneous mutagenesis of a plant potyvirus genome after insertion of a foreign gene. *J Virol* 67:5968–5975

Escriu F, Perry KL, García-Arenal F (2000) Transmissibility of Cucumber mosaic virus by Aphis gossypii Correlates with Viral Accumulation and Is Affected by the Presence of Its Satellite RNA. *Phytopathology* 90:1068–1072

Fenton A, Magoolagan L, Kennedy Z, Spencer KA (2011) Parasite-induced warning coloration: a novel form of host manipulation. *Anim Behav* 81:417–422

Fereres A (2007) Aphid Behavior and the Transmission of Noncirculative Viruses. In: Brown JK (ed) Vector-Mediated Transmission of Plant Pathogens. The American Phytopathological Society, pp 31–45

Fredeen AL, Rao IM, Terry N (1989) Influence of phosphorus nutrition on growth and carbon partitioning in Glycine max. *Plant Physiol* 89:225–230

Galigniana MD, Morishima Y, Gallay PA, Pratt WB (2004) Cyclophilin-A is bound through its peptidylprolyl isomerase domain to the cytoplasmic dynein motor protein complex. *J Biol Chem* 279:55754–55759

Hagen SB, Folstad I, Jakobsen SW (2003) Autumn colouration and herbivore resistance in mountain birch (Betula pubescens). *Ecol Lett* 6:807–811

Hamilton WD, Brown S. (2001) Autumn tree colours as a handicap signal. *Proc R Soc London Ser B* 268:1489–1493

Harris KF (1977) An ingestion-egestion hypothesis of noncirculative virus transmission. In: Aphids As Virus Vectors. Elsevier, pp 165–220

Jakobs R, Müller C (2018) Effects of intraspecific and intra-individual differences in plant quality

on preference and performance of monophagous aphid species. *Oecologia* 186:173–184

Katis NI, Maliogka VI, Dovas CI (2012) Viruses of the Genus Allium in the Mediterranean Region. In: Advances in Virus Research. Academic Press Inc., pp 163–208

Kennedy JS, Day MF, Eastop VF (1961a) A Conspectus of Aphids as Vectors of Plant Viruses. London, Commonw. Inst. Ent. London pp114

Kennedy JS, Kershaw WJSS, Booth CO, Kershaw WJSS (1961b) Host finding by aphids in field. III. Visual attraction. *Ann Appl Biol* 49:1–21

Kim H, Aoki N, Takahashi H, Yoshida N, Shimura H, Masuta C (2020) Reduced RNA silencing suppressor activity of onion yellow dwarf virus HC-Pro with N-terminal deletion may be complemented in mixed infection with another potyvirus in garlic. *J Gen Plant Pathol* 86:1–10

López-Moya JJ (2002) Genes involved in insect-mediated transmission of plant viruses. In: Khan, J.A., Dijkstra J (ed) Plant Viruses as Molecular Pathogens. Food Products Press, NY, pp 31–61

Lot H, Chovelon V, Souche S, Delecolle B (1998) Effects of onion yellow dwarf and leek yellow stripe viruses on symptomatology and yield loss of three French garlic cultivars. *Plant Dis* 82:1381–1385

Lupetti P, Mencarelli C, Rosetto M, Heuser JE, Dallai R (1998) Structural and molecular characterization of dynein in a gall-midge insect having motile sperm with only the outer arm. *Cell Motil Cytoskeleton* 39:303–317

Macias W, Mink GI (1969) Preference of green peach aphids for virus-infected sugarbeet leaves. *J Econ Entomol* 62:28–29

Manglli A, Mohammed HS, El Hussein AA, Agosteo GE, Albanese G, Tomassoli L (2014)

Molecular analysis of the 3' terminal region of Onion yellow dwarf virus from onion in southern Italy. *Phytopathol Mediterr* 53:438–450

Masuta C, Hayashi Y, Wang WQ, Takanami Y (1990) Comparison of Four Satellite RNA Isolates of Cucumber Mosaic Virus. *Japanese Journal of Phytopathology*, *56*(2):207-212.

Masuta C, Suzuki M, Matsuzaki T, Honda I, Kuwata S, Takanami Y, Koiwai A (1993) Bright yellow chlorosis by cucumber mosaic virus Y satellite RNA is specifically induced without severe chloroplast damage. *Physiol Mol Plant Pathol* 42:267–278

Mittler TE, Dadd RH (1962) Artificial feeding and rearing of the aphid, Myzus persicae (Sulzer), on a completely defined synthetic diet. *Nature* 195:404

Mohammed HS, Zicca S, Manglli A, Elaiderous Mohamed M, El Siddig MAR, El Hussein AA, Tomassoli L (2013) Occurrence and phylogenetic analysis of potyviruses, carlaviruses and allexiviruses in garlic in Sudan. *J Phytopathol* 161:642–650

Morazzani EM, Wiley MR, Murreddu MG, Adelman ZN, Myles KM (2012) Production of Virus-Derived Ping-Pong-Dependent piRNA-like Small RNAs in the Mosquito Soma. *PLoS Pathog* 8:e1002470

Paula DP, De Souza LM, Andow DA, De Sousa AATC, Pires CSS, Sujii ER (2016) Artificial tritrophic exposure system for environmental risk analysis on aphidophagous predators. *An Acad Bras Cienc* 88:1569–1575

Pinheiro P V., Wilson JR, Xu Y, et al. (2019) Plant Viruses Transmitted in Two Different Modes Produce Differing Effects on Small RNA-Mediated Processes in Their Aphid Vector. *Phytobiomes* J 3:71–81

Pirone TP, Blanc S (1996) Helper-dependent vector transmission of plant viruses. *Annu Rev Phytopathol* 34:227–247

Pirone TP, Harris KF (1977) Nonpersistent transmission of plant viruses by aphids. *Annu Rev Phytopathol* 15:55–73

Pitrat M (2012) Vegetable Crops in the Mediterranean Basin with an Overview of Virus Resistance. In: Advances in Virus Research. Academic Press Inc., pp 1–29

Raccah B, Huet H, Blanc S (2001) Potyviruses. In: Harris KF, Smith OP, Duffus JE (eds) Virus-Insect-Plant Interactions. Academic Press, 10-Potyviruses, pp 181–206

Roossinck MJ (2005) Symbiosis versus competition in plant virus evolution. *Nat Rev Microbiol* 3:917–924

Sabin LR, Zheng Q, Thekkat P, Yang J, Hannon GJ, Gregory BD, Tudor M, Cherry S (2013) Dicer-2 Processes Diverse Viral RNA Species. *PLoS One* 8:e55458

Schnettler E, Donald CL, Human S, Watson M, Siu RWC, McFarlane M, Fazakerley JK, Kohl A, Fragkoudis R (2013) Knockdown of piRNA pathway proteins results in enhanced semliki forest virus production in mosquito cells. *J Gen Virol* 94:1680–1689

Shang, F., Niu, J., Ding, B.Y., Zhang, W., Wei, D.D., Wei, D., Jiang, H.B. and Wang, J.J., 2020. The miR-9b microRNA mediates dimorphism and development of wing in aphids. *Proceedings of the National Academy of Sciences*, *117*(15):8404-8409.

Shimura H, Pantaleo V, Ishihara T, Myojo N, Inaba J, Sueda K, Burgyán J, Masuta C (2011) A Viral Satellite RNA Induces Yellow Symptoms on Tobacco by Targeting a Gene Involved in Chlorophyll Biosynthesis using the RNA Silencing Machinery. *PLoS Pathog* 7:e1002021

Simon AE, Roossinck MJ, Havelda Z (2004) Plant virus satellite and defective interfering RNAs: new paradigms for a new century. *Annu Rev Phytopathol* 42:415–452

Song X-S, Wang Y-J, Mao W-H, Shi K, Zhou Y-H, Nogué S, Yu J-Q (2009) Effects of cucumber mosaic virus infection on electron transport and antioxidant system in chloroplasts and

mitochondria of cucumber and tomato leaves. *Physiol Plant* 135:246–257

Sparkes TC, Wright VM, Renwick DT, Weil KA, Talkington JA, Milhalyov M (2004) Intra-specific host sharing in the manipulative parasite Acanthocephalus dirus: does conflict occur over host modification? *Parasitology* 129:335–40

Sylvester ES (1956) Beet Yellows Virus Transmission by the Green Peach Aphid. *J Econ Entomol* 49:789–800

Takaki F, Sano T, Yamashita K (2006) The complete nucleotide sequence of attenuated onion yellow dwarf virus: A natural potyvirus deletion mutant lacking the N-terminal 92 amino acids of HC-Pro. *Arch Virol* 151:1439–1445

Tsuchida T, Koga R, Horikawa M, Tsunoda T, Maoka T, Matsumoto S, Simon JC, Fukatsu T (2010) Symbiotic bacterium modifies aphid body color. *Science* 330:1102–1104

Tungadi T, Groen SC, Murphy AM, Pate AE, Iqbal J, Bruce TJA, Cunniffe NJ, Carr JP (2017) Cucumber mosaic virus and its 2b protein alter emission of host volatile organic compounds but not aphid vector settling in tobacco. *Virol J* 14:91

Van Dijk P (1996) Survey and characterization of potyviruses and their strains of Allium species. *Netherlands J Plant Pathol* 99:1–48

Wang IN, Yeh W Bin, Lin NS (2017) Phylogeography and coevolution of bamboo mosaic virus and its associated satellite RNA. *Front Microbiol* 8:886

Ward LI, Perez-Egusquiza Z, Fletcher JD, Clover GRG (2009) A survey of viral diseases of Allium crops in New Zealand. *Australas. Plant Pathol.* 38:533–539

Watson MA, Roberts FM (1939) A comparative study of the transmission of Hyoscyamus virus 3, potato virus Y and cucumber virus 1 by the vectors *Myzus persicae* (Sulz), *M. circumflexus* (Buckton), and *Macrosiphum gei* (Koch). *Proc R Soc London Ser B - Biol Sci*

127:543–576

Webster CG, Pichon E, van Munster M, Monsion B, Deshoux M, Gargani D, Calevro F, Jimenez J, Moreno A, Krenz B, Thompson JR, Perry KL, Fereres A, Blanc S, Uzest M (2018) Identification of plant virus receptor candidates in the stylets of their aphid vectors. *J Virol* 92:14

Westwood JH, Groen SC, Du Z, Murphy AM, Anggoro DT, Tungadi T, Luang-In V, Lewsey MG, Rossiter JT, Powell G, Smith AG, Carr JP (2013) A trio of viral proteins tunes aphid-plant interactions in arabidopsis thaliana. *PLoS One* 8:1–18

Wu D, Qi T, Li W-X, Tian H, Gao H, Wang J, Ge J, Yao R, Ren C, Wang X-B, Liu Y, Kang L, Ding S-W, Xie D (2017) Viral effector protein manipulates host hormone signaling to attract insect vectors. *Cell Res* 27:402–415

Wu Q, Luo Y, Lu R, Lau N, Lai EC, Li WX, Ding SW (2010) Virus discovery by deep sequencing and assembly of virus-derived small silencing RNAs. *Proc Natl Acad Sci U S A* 107:1606–1611

Wyatt IJ, White PF (1977) Simple Estimation of Intrinsic Increase Rates for Aphids and Tetranychid Mites. *J Appl Ecol* 14:757

Yang X, Thannhauser TW, Burrows M, Cox-Foster D, Gildow FE, Gray SM (2008) Coupling genetics and proteomics to identify aphid proteins associated with vector-specific transmission of polerovirus (luteoviridae). *J Virol* 82:291–299

Ziebell H, Murphy AM, Groen SC, Tungadi T, Westwood JH, Lewsey MG, Moulin M, Kleczkowski A, Smith AG, Stevens M, Powell G, Carr JP (2011) Cucumber mosaic virus and its 2b RNA silencing suppressor modify plant-aphid interactions in tobacco. *Sci Rep* 1:187

ACKNOWLEDGEMENT

I sincerely express my gratitude to my supervisor, Professor Chikara Masuta, Pathogen-Plant Interaction Laboratory, Hokkaido University for his unstinted support. His infinite passion on research, style of student supervision and kind words, always motivated me to become a scientist like him.

I am truly thankful to Prof. Akimoto Shin-ichi, Laboratory of Systematic Entomology, Hokkaido University and Dr. Hanako Shimura, Laboratory of Crop Physiology, Hokkaido University for their detailed review and valuable comments given to improve my thesis.

I also truly grateful to Dr Kenji Nakahara, Pathogen-Plant Interaction Laboratory, Hokkaido University for his kind advice and assistance rendered me during this period.

I specially thank Dr. Hangil Kim for his guidance and being a wondaful colleague and a friend. Further, I would like to extend my sincere thanks to all my labmates at Pathogen-Plant Interaction Laboratory, who extended their support whenever I needed.

I always thank my parents for supporting everything in my life and want to convey my deepest gratitude to Dineesha and Shevi, whom has always been and will be the strength of my life.